CA/DOH/AIHL/SP-40

DRY DEPOSITION OF ACIDIC GASES AND PARTICLES

FINAL REPORT
Prepared for the California Air Resources Board
Interagency Agreement A3-108-32

February 1986

Walter John, Stephen M. Wall, Joseph L. Ondo and Hwa-Chi Wang
Air and Industrial Hygiene Laboratory
California Department of Health Services
2151 Berkeley Way
Berkeley, California 94704

Submitted to: John Holmes, Ph.D., Chief
Research Division
California Air Resources Board
P.O. Box 2815
Sacramento, California 95812

"The statements and conclusions in this report are those of the contractor and not necessarily those of the California Air Resources Board. The mention of commercial products, their source or their use in connection with material reported herein is not to be construed as either an actual or implied endorsement of such products".

CONTENTS

ABSTRACT

Several techniques have been developed for the measurement of dry acid deposition. The deposition of particulate sulfate and nitrate on leaves, pine needles and surrogate surfaces was measured directly by washing off the deposits. Deposition velocities were derived from parallel sampling of airborne particle concentrations. Surface exposures ranging from 14 to 62 days under nearly unvarying meteorological conditions gave constant deposition velocities. Deposition velocities were approximately the same for all surfaces and somewhat higher for nitrate compared to sulfate. Surrogate surfaces had deposits on the top surface only. A surrogate Nuclepore "leaf" sampled sulfur dioxide at a rate consistent with a bubbler but much higher than predicted. The bubbler performed well, even under extreme conditions.

A method was validated for the measurement of the size distributions of acidic particles. The Berner cascade impactor was calibrated with monodisperse aerosols. A Halocarbon grease compatible with acid analysis was shown to suppress particle bounce. It was shown that ammonium sulfate particles are properly sized, even at high relative humidities. Evaporative losses of ammonium nitrate reach only 7% at 35°C. Ambient size distributions of strong acid, sulfate, nitrate, ammonium, sodium and chloride ions were measured at Oildale and Berkeley. Distributions vary between species and with ambient conditions.

I. Introduction

The dry deposition of acidic gases and particles is of special concern in semi-arid California. Assessment of the possible impact of dry acid deposition on the environment requires the use of appropriate measurement methods which, however, are still under development because dry deposition is a complex process that is incompletely understood.

The present work is Phase III of a multi-year program funded by the Kapiloff Acid Deposition Act of 1982. The objectives of the program are:

1. To study the mechanisms of dry deposition in order to provide a better basis for monitoring methods.
2. To develop measurement techniques suitable for long term monitoring of dry acid deposition.
3. To make baseline measurements of dry acid deposition at representative sites in California.

Phase I

The ambient concentration method was selected for the development of monitoring techniques for dry acid deposition. All of the major acidic gas and particle species were sampled by methods designed to minimize artifacts, volatilization losses and interferences. Other pollutants and meteorological parameters were monitored. Sampling was conducted at Martinez, San Jose and Democrat Springs (Kern River canyon east of Bakersfield).

The results, which have been reported (1), established baseline values of ambient concentrations of acidic pollutants at these California locations and data on their diurnal variations. Redundant sampling and ion balances confirmed the quantitative accuracy of the sampling techniques.

Phase II

The baseline measurements of acidic pollutant concentrations were extended to the important Los Angeles basin (2-5). The highest acid concentrations were detected at Tanbark Flats, representative of vulnerable forested mountain areas

downwind of Los Angeles. Particle size distributions were obtained for specific chemical species including hydrogen ion, the first such data available. Over 50% of the nitrate at West Los Angeles was larger than 2.5 μm. This is significant since the deposition velocity increases rapidly with particle size.

Deposition velocities were measured for sulfate and nitrate depositing on leaves of two species of Ligustrum and on surrogate surfaces. Exploratory measurements were made with a thin iron film detector for sulfuric acid droplets and a Nuclepore surrogate "leaf" for sulfur dioxide.

A preliminary recommendation was made for a practical sampling scheme capable of monitoring the major acidic gases and particles.

Phase III

This phase is the subject of the present report. The objectives include:

1. Field testing of a bubbler sampler for sulfur dioxide.
2. Direct measurements of acidic particle deposition on leaves of Ligustrum, pine needles and surrogate surfaces.
3. Further testing of a Nuclepore surrogate "leaf" as a passive sampler for sulfur dioxide which could be deployed in a plant canopy.
4. Validation of the techniques for measurement of acidic particle size distributions and additional ambient measurements.

These diverse topics have the common objective of providing measurement methods and baseline data on dry acid deposition in California.

II. Dry Deposition Measurements at Oildale

The Air Resources Board air monitoring station at Oildale (adjacent to Bakersfield) was selected for testing of the SO_2 bubbler, the Nuclepore passive sampler and for measurements of particle deposition on leaves and surrogate surfaces. This site was chosen because SO_2 concentrations are typically among the highest in California. The site also satisfied the requirement of a minimum chance of rainfall to permit long term accumulation of particles on the leaves. The experiments were conducted from August 3 to October 18, 1984.

Experimental Arrangement

The site is located on the edge of a residential district near the oil field. A chain link fence encloses an area on dry ground. The AIHL Mobile Laboratory (1) was parked next to the ARB station. Figure 1 diagrams the layout.

Meteorological instruments were mounted on a mast on the mobile laboratory. Wind speed, wind direction, temperature and dew point were continuously recorded by an Apple II computer system. Figures 2 and 3 shows these variables during a typical week of the study.

Site visits were made weekly to change the Monocut filter and the bubbler solutions, harvest leaves and perform maintenance.

Bubbler Sampling of SO_2

Ambient concentrations of SO_2 in the 1 ppb range are significant for dry deposition. However, electronic monitors for SO_2 are reliable only above 5-10 ppb. A bubbler containing a 0.1N solution of hydrogen peroxide to oxidize the SO_2 to sulfate is a simple sampler with the required sensitivity. It has been suggested (6,7) that this method replace the West-Gaeke method as the EPA reference method for SO_2 because the West-Gaeke method suffers from temperature effects.

The present work extends our previous experience (1,2) with bubblers. Week long runs under the extremely high temperatures and low relative humidity presented a worst case test. Indeed, during the first three weeks some of the bubblers ran dry. This problem was overcome by placing a third bubbler in series with the usual two and later, by using a larger 200 mL bubbler followed by two normal 40 mL bubblers (Figure 4). Aluminum foil was used as a sun shield. The bubbler was operated at a flow rate of 0.5 L/min. The hydrogen peroxide solutions were refrigerated before and after use in the bubbler. Sulfate and nitrate were quantitated by ion chromatography.

The SO_2 concentration measured by the bubbler averaged 7.5 $\pm$ 0.3 ppb over the entire experiment. The quoted uncertainty is the standard deviation of the

values for individual measurement periods. A similar degree of constancy was exhibited by most of the other measured variables (Table 1). Although this concentration is very significant for acid deposition, it is below the stable range of electronic monitors. The SO_2 concentrations from the bubbler averaged 0.9 $\pm$ 0.4 times that of the ARB monitor, which is near unity but the uncertainty is too large to provide a useful test of the bubbler.

The nitrate in the bubbler solutions is presumably from absorbtion of oxides of nitrogen. Nitric acid may also contribute to the nitrate. The ratio of the bubbler nitrate to that expected from NO_x measured by the ARB monitor was 0.20 $\pm$ 0.04. The low ratio may result from the relatively low solubility of NO_x.

Dry Deposition of Particulate Sulfate and Nitrate on Leaves and Surrogate Surfaces

A direct measurement of dry deposition of acidic particles on leaves can be made by washing off the deposit and analyzing the extract. If the ambient particle concentration is measured during the exposure, deposition velocities can be derived. In previous work (2,5) we have demonstrated the feasibility of this technique, using potted plants of Ligustrum. The potted plants can be transported to different sites for comparison of deposition under different conditions. The object of the present work was to measure deposition in Oildale, to investigate the effect of exposure duration on the derived deposition velocities and to extend the technique to pine needles, since large areas of California are covered with conifers. As in the past, we also exposed plastic surrogate surfaces for comparison. The top and bottom surfaces can be analyzed separately, providing useful information on the deposition process. Details of extraction and analysis procedures have been given previously (2).

Ambient Concentrations of Sulfate and Nitrate

Ambient particle concentrations are needed for the determination of deposition velocities. Three filter samplers were operated at the site, our Monocut sampler and the ARB station's Hivol and PM_{10} sampler (Hivol with Size-selective Inlet). The Monocut (Sierra Instruments) consisted of the original 15 µm Dichotomous

sampler inlet connected directly to a 37 mm filter holder. It was initially operated at 1 L/min to allow 7 day unattended operation. During the second half of the study, the flow rate was increased to 1.9 L/min. The particle size cutpoint is uncertain because the design flow rate is 16.7 L/min. However, both sulfate and nitrate particles are expected to be considerably smaller than the cutpoint. The 2 μm pore size Teflon membrane filter was analyzed for sulfate and nitrate by ion chromatography. The ARB Hivol was operated with a glass fiber filter and the Size-selective Inlet (SSI) sampler was operated with a quartz filter.

While the Monocut was operated continuously, the Hivol and SSI were run for 24 hours every six days. A comparison was made between concentrations averaged over approximately one month. The periods differ by a few days because of unsynchronized schedules; however, this should have only a minor effect on the comparison because the weekly averages were remarkably constant. The data are summarized in Table 2.

The comparison is a striking example of the differing sampling characteristics of filter media. For sulfate, the Monocut and SSI agree within 2%, but the Hivol is a factor of two higher. Glass fiber filters are known to have an appreciable efficiency for sampling sulfur dioxide (8), which accounts for the high sulfate value from the Hivol. The additional sulfate corresponds to a collection efficiency for sulfur dioxide of about 25%. For determination of sulfate deposition velocities the Monocut sulfate concentrations were used.

Both the Monocut and SSI collected much less nitrate than the Hivol, attributable to volatilization losses of ammonium nitrate from the Teflon and Quartz media (8). Losses of this magnitude from Teflon filters have been observed previously. The Monocut losses were smaller than those of the SSI, probably because of the much lower face velocity. The Hivol's glass fiber filter does not lose ammonium nitrate because the resulting nitric acid is efficiently collected by glass fiber. This also implies that the Hivol nitrate is high because ambient nitric acid is sampled. This error depends on the nitric acid concentrations; however, we expect this error to be smaller than that from the volatilization losses, especially for long-term averages since nitric acid concentrations are near zero at night. Therefore, nitrate deposition velocities below are calculated from the Monocut

nitrate, but corrected by the overall ratio of Hivol to Monocut nitrate. To the extent that nitric acid contributes to the Hivol nitrate, the calculated nitrate deposition velocities will be underestimated; the error is probably in the range of 10-30%.

Deposition Velocities vs. Exposure Duration

Atmospheric conditions and pollutant concentrations were remarkably constant during the first 62 days of the study, as shown in Table 1. The two weeks immediately following had periods of trace to light rains and cooler temperatures. Therefore data were used from the first 62 days only. The constancy of conditions permits a comparison of the deposition velocities derived from exposures ranging from 6 to 62 days. This set of data was generated by washing the plants, then harvesting leaves at intervals. Figure 5 shows that, with the exception of the shortest exposure (6 days), the deposition velocities are independent of exposure time. Tables 3 and 4 show that the deposition velocities from 6 or 7 day exposures are sometimes higher than those from longer exposures. This is seen for both sulfate and nitrate and for natural and surrogate surfaces. We have no explanation for this effect. The data indicate that very consistent results can be obtained for periods of 14-62 days.

Using another set of plants, exposures of shorter duration (1-3 weeks) were carried out during the above 62 day period. Examination of these data show that the deposition velocities were somewhat lower during the last two weeks of the study, averaging 40% lower for nitrate and 30% lower for sulfate (averaged over all surfaces). During the last two weeks the weather was beginning to change and the temperature averaged cooler by $5^{o}C$. There was no significant change in any other variable.

Deposition Velocities of Particulate Sulfate and Nitrate

Deposition velocities for sulfate are listed in Table 3 and for nitrate in Table 4. It should be noted that the deposition velocities for the surrogate surfaces are based on the top surface only whereas the deposition velocities for leaves and pine needles involve the total surface area. Ratios of deposition velocities on surrogate surfaces to those on leaves are listed in Table 5. The consistently

lower values for L. ovalifolium may be due to the leaf geometry. The leaves tend to fold along the long axis, the amount depending on sunlight, humidity and other conditions. We measured the flat area of the leaves; however, folding reduces the projected area. For example, a 60^{o} included angle (not untypical) reduces the projected area a factor of two. This would bring the deposition velocity for L. ovalifolium into rough agreement with those for L. japonicum and surrogate surfaces. The surface areas of the pine needles were calculated from a formula (Paul Miller, private communication) which uses the length and diameter as input parameters. The deposition velocities for sulfate on P. coulteri are somewhat high, but the standard deviation is large. Therefore, overall, all the surfaces, natural and surrogate, collect particles at roughly the same rate (Table 5).

For the surrogate surfaces it was possible to separate deposition on the top from that on the bottom surface. The tables show that in no case was any significant deposit found on the bottom surface except for the Nuclepore "leaves" containing peroxide, which collected sulfate but not nitrate on the bottom surface. Probably the peroxide solution passed through the filter pores (which were on the bottom) and wetted the bottom surface which subsequently absorbed gaseous sulfur dioxide. Therefore, there is no evidence that particles deposited on the bottom surfaces.

That 30 to 40% larger deposition velocities are observed for nitrate compared to sulfate is not unreasonable since nitrate particles have an appreciable coarse component whereas sulfate particles are predominately submicron. The deposition velocity increases rapidly with particle size above 1 μm.

The deposition velocities for Oildale are compared in Table 6 to those measured in West Los Angeles and Tanbark Flats in August, 1983 (2,5). The 6-7 day Oildale exposures were compared to the 4 day exposures in Los Angeles and Tanbark. The Oildale deposition velocities on leaves are generally higher but are about the same for surrogate surfaces.

SO_2 and NO_x Sampling with Nuclepore "Leaves"

SO_2 and NO_x deposit in leaves through the stomata. We have already reported (2,5) some preliminary experiments with a surrogate leaf constructed of several

materials in a 2 x 2 inch plastic film slide holder (Figure 6). The gases diffuse through the pores of the Nuclepore filter to a wet cellulose filter. The interior surfaces are extracted and analyzed by ion chromatography.

The surrogate leaf is a passive sampler which can be placed in a canopy for a period limited only by the drying out time, a week or more, depending on the temperature and relative humidity. Oildale presented an extreme case of dry heat, causing filters to dry out in less than a week. A second model of the surrogate leaf was constructed with a larger wick and a larger water reservoir. This increased the time to dryness, but the larger model collected sulfate and nitrate at a rate smaller by a factor of 3 to 4. Therefore, results are not reported for the larger model. To reduce the rate of water loss, the surrogate leaves were placed under a sunshade. This solved most of the problems; however, the filters still showed some dry spots. Since the sunshade was open on all sides, it should not have affected the sampling of gases. Indeed, the observed deposition of particles on the top surface of the surrogate leaves showed no significant change associated with the sunshade.

Almost all of the sulfate and nitrate was found in the cellulose filter; much less was in the reservoir. In one run only, 34% was in the reservoir; in all other runs the reservoir content was negligible. The internal deposition rates for sulfate and nitrate are listed in Table 7 for the various types of surrogate leaves. These include an 8 µm pore size and a double Nuclepore filter version with 0.03 and 0.05 µm pore sizes in series. Some data was taken with a 0.1N hydrogen peroxide solution instead of water in the cellulose filter and reservoir to see if enhanced oxidation of SO_2 to SO_4 would affect the collection rate.

The peroxide solution increased the deposition rate by a small factor, but introduced other problems, including increased sulfate deposition on the bottom external surface of the "leaf". The peroxide solution also sampled organic acids. For these reasons, the peroxide was not considered an improvement. Compared to the bubbler, the Nuclepore leaf (8 µm pore size, water solution) sampled at a relative rate of 0.10 $\pm$ 0.03 for sulfate and 0.08 $\pm$ 0.01 for nitrate. Therefore the effective sampling rate of the Nuclepore leaf was 0.05 L/min. In other terms, the deposition velocity for SO_2 was 0.21 $\pm$ 0.04 cm/s and for NO_x, 0.06 $\pm$ 0.03 cm/s, which are very close to the deposition velocities measured at Tanbark, 0.24 and 0.05 cm/s respectively.

Comparison to Diffusion Theory

SO_2 and NO_x diffuse into the Nuclepore "leaf" while water vapor diffuses out. The latter will be discussed first since the result is significant for the former. Water loss was high under the high temperatures and low humidity prevailing at Oildale. We will compare the calculated rate of water loss to measurements made earlier at West Los Angeles and Tanbark Flats.

The water diffuses from the saturated cellulose filter through the separating screen and the Nuclepore filter to the outside. The rate of mass transfer is given by Fick's Law:

$$\frac{dm}{dt} = (D (1 - RH) CA) / L \qquad (1)$$

where D is the diffusion coefficient of water vapor (taken to the 0.239 cm^2/sec), RH is the relative humidity (fractional) and C is the concentration of water vapor in air saturated at the ambient temperature. A is the area and L the length of a diffusion channel equivalent to that of the Nuclepore leaf. For 8 µm pore size Nuclepore followed by the Teflon screen with 35% open area and thickness of 0.055 cm, A/L = 0.24 cm.

The ambient temperature and relative humidity vary diurnally, the maximum temperature and minimum relative humidity occuring at the same time and vice versa (See Figure 2). As an estimate of the average, we calculated the loss rates at the two extrema and took the geometric mean. The ambient data and results of the water loss calculation are listed in Table 8. The theory underestimates the loss rate by a large factor. A probable explanation of the discrepancy is that the air inside the "leaf" is saturated with water vapor. This would reduce the diffusion length from the 0.055 cm thickness of the screen to the 8.8 µm thickness of the Nuclepore filter. The loss rate would be increased by a factor of 63, bringing the calculated result into reasonable agreement with that measured (last column, Table 8).

The mass rate of sampling of SO_2 and NO_x were also calculated from Fick's Law, Equation (1) without the RH term and C the concentration of the gas. The calculated result for NO_x is further multiplied by 0.20, the observed fraction of NO_x converted to nitrate in the bubbler.

The ratios of measured to theoretical rates of sampling for SO_2 and NO_x are listed in Table 9 for three locations. The mean ratios for SO_2 and NO_x are in agreement, both being about 5. The explanation for this factor of 5 is probably that the surfaces of the screen were wet, reducing the diffusion distance. It is necessary, however, to explain why the effect is much smaller for gases. This may be because the gases must diffuse considerably farther than just the thickness of the Nuclepore filter before sufficient wet surface area is encountered to absorb the gases.

Additional evidence of effects produced by the outward streaming of water vapor is afforded by the sulfate found on the bottom (outside) surface of the "leaves" containing peroxide solution. No sulfate was found on the bottom when pure water was used, showing that the peroxide was transported from inside the "leaf" to the bottom surface where it oxidized a detectable amount of SO_2.

Theoretically, the 0.03 + 0.05 µm surrogate leaf should sample much slower than the 8 µm pore leaf, but instead it samples at almost the same rate (Table 7). It is not profitable to attempt an explanation of this even more complicated "leaf". The experimental result shows that this version of the leaf offers no advantages.

III. Size Distributions of Ambient Acidic Particles

The deposition velocities of acidic particles depend strongly on particle size (9). In preliminary work (2,4), we have shown that size distributions of individual acidic species can be measured with the Berner cascade impactor (10); in fact, size distributions of strong acid were obtained for the first time. To confirm and extend these results requires investigation of the general sampling characteristics of the Berner impactor as well as specific effects associated with the

acidic species of interest. The necessary research has been conducted under controlled conditions using laboratory-generated aerosol and with ambient aerosol in field sampling.

Sampling Characteristics of the Berner Impactor

Cascade impactors are widely used to fractionate airborne particles according to aerodynamic size for subsequent chemical analysis. By reducing the pressure, it is possible to extend the classifying capability of the cascade impactor down to cover the submicron particles in the ambient accumulation mode, as demonstrated by Hering, et al. (11). Unfortunately, the flow rate in the Hering impactor is inadequate for the analysis of particulate acid. Recently, a high flow rate, low pressure impactor was designed by Berner and used in field studies by Berner, et al. (10). The Berner impactor (Figure 7) has some favorable sampling characteristics including sharp cutoffs and low wall losses.

Because detailed information on the performance of the Berner impactor was unavailable, it was necessary to calibrate the impactor with well defined laboratory aerosols. The calibration of the submicron stages, in particular, required development work to produce the necessary aerosol. The stage sampling efficiencies and wall losses were determined. Particle bounce and its suppression with greased impaction surfaces was investigated. The effects of the high jet velocities on liquid particles was studied. Ammonium sulfate aerosol was generated to examine the possible effects of humidity including growth by condensation when the jet expansion occurs and the effect on the sticking probability. Ammonium nitrate aerosol was used to investigate volatility losses in the low pressure environment.

Flow Calibration

The design parameters of the Berner impactor are listed in Table 10. The first six columns were given by Berner, et al. (10) based on a flow rate of 30 L/min. Note that the sequence of stage numbers is opposite to the usual convention, stage 1 being the last stage, the stage collecting the smallest size fraction. The flow rate is controlled by a critical orifice located downstream of stage 1.

We calibrated the volumetric flow rate of the impactor against a dry gas meter and found it to be within 2% of the designed value. However, certain precautions had to be observed, as explained below. The maximum mass flow rate, G, is limited by the critical orifice (12):

$$G = A\left[2/(K+1)^{1/(K-1)}\right]\left(\frac{2K}{K+1}\right)\rho_1 P_1)^{\frac{1}{2}} \qquad (2)$$

where A is the effective area of the critical orifice, K is the specific heat ratio of air, P_1 and ρ_1 are the air pressure and density at stage 1. The mass flow rate conserves and varies linearly with volumetric flow rate, Q, assuming incompressible flow. With P/ρ^K = constant, we have:

$$Q \propto P_1^{(K+1)/2K} \qquad (3)$$

Since the stage pressures decrease with each successive stage, the absolute pressure at stage 1 (P_1) is affected by any changes in pressure occuring in the upper stages. For example, if the nozzles are clogged on any stage, P_1 will be decreased and a lower flow rate will result. If the vacuum pump does not have enough capacity to reach the critical pressure ratio of 0.53, the orifice will not be operated at the critical condition and a further reduction of flow rate will occur. If leakage occurs at any stage, P_1 will increase and a higher flow rate will result. Our experience is that significant leakage occurs if the impactor is not carefully assembled and tightened. A valuable check on the flow condition is afforded by installing a vacuum gauge downstream of the orifice. If the pressure is less than 5 in. of Hg, we find the flow rate to be within 2% of the designated value. When the system is leaking, the pressure is higher. For example, a pressure of 5.4 in. of Hg corresponds to a flow rate of 35 L/min.

The nozzle velocities given in column 5 of Table 10 are calculated assuming incompressible flow for stages 6-9 and compressible flow for stages 1-5. The compressible flow is for a straight nozzle with an empirical correction factor to account for the non-ideal flow condition (10). These nozzle velocities were used by Berner to calculate the 50% cutoff particle diameters listed in column 6 for a Stokes number of 0.22 based on the theory of Marple and Liu (13). A

more accurate calculation by Rader and Marple (14) gives a Stokes number of 0.24 for 50% efficiency. The corresponding cutoff diameters are given in column 7.

Calibration of the Upper Stages

Two very different techniques are required to generate super vs. submicron particles. In this section, the calibration of the upper stages (5-8) are described. Stage 9 is not included since it is used only to prevent coarse particles from entering the impactor and not for collecting samples.

Monodisperse aerosols with a geometric standard deviation better than 1.03 were produced with the vibrating orifice aerosol generator (15). The particle diameter can be calculated directly from the generator's operating parameters. The aerosol was continuously monitored by an optical counter (Climet 201) and a pulse height analyzer. Doublet and triplet counts from coagulated particles were typically 0.3% and 0.005% of the singlet count respectively and could therefore be neglected. Liquid particles were generated, consisting of oleic acid tagged with 1% uranine. The material collected on each stage substrate (Tedlar foil) was extracted with water and quantitated on a fluorometer. The critical orifice in the exhaust of the impactor prevented the use of an after filter; however, it can be safely assumed that these large particles did not penetrate completely through the impactor.

The collection efficiency E_n of stage n is determined from:

$$E_n = M_n / \left(\sum_{i=1}^{n} M_i\right) \qquad (4)$$

where M_n is the particle mass collected on stage n. The measured efficiency is plotted against the aerodynamic diameter in Figure 8. It can be seen that the cutoffs are fairly sharp. The corresponding 50% cutoff diameters are listed in column 8 of Table 10. For stages 6 to 8, the 50% cutoff diameter agrees with the adjusted theoretical prediction (column 7, Table 10) within 2%. However, the measured value for stage 5 is 8% smaller than the theory predicts. This stage has a large number of nozzles (50). A trace of deposition in the form

of a line between adjacent spots was observed. Evidently the stagnation zone between the closely spaced jets causes additional deposition, resulting in a shift of the cutoff curve to smaller diameters.

The wall loss was determined by washing all of the inner surfaces of the impactor after each day's experiments. The average wall loss was determined to be 1.1% for particles larger than 2 μm and 3.0% for particles between 0.5 and 2 μm. Since the losses are small and are for the worst case represented by liquid particles, they can be neglected in the efficiency calculations.

Calibration of Lower Stages

No standard technique is available to generate monodisperse submicron aerosol for use with dye tracers. The atomization-electrostatic classification method (16) can produce aerosol with a geometric standard deviation of 1.05; however, a small fraction of doubly charged particles with twice the diameter is included. A typical doublet number fraction of 10% would contribute 40% of the mass. To overcome this problem, we adjusted the peak of the aerosol size entering the electrostatic classifier to be well below that selected by the classifier. Thus the classifier is selecting particles from a distribution which is decreasing rapidly with size, suppressing the doublets.

Preliminary measurements with liquid oleic acid aerosol encountered some anomalous effects on stages 1 and 2 associated with high jet shear forces on the liquid. Because of the importance of assessing these effects, a separate investigation with liquid aerosol was carried out, and is presented later in this report. For the stage calibrations, we developed a suitable aerosol consisting of solid ammonium fluorescein particles coated with oleic acid to prevent bounce.

The experimental arrangement is diagrammed in Figure 9. A mixture of 95% fluorescein - 5% oleic acid in 75% ammonium hydroxide - 25% isopropyl alcohol solvent was fed to a constant output atomizer (TSI 3075) by an HPLC pump (Rabbit, Rainin Instruments) to provide a very constant feed rate over an entire day. The solvent and oleic acid were evaporated in a tube furnace operating at 200°C. The aerosol-vapor mixture was then directed to a chamber to allow the oleic acid vapor to condense on the solid ammonium fluorescein particles.

Hot, dry, particle-free sheath air was used to surround the mixture at the entrance to the condensation chamber to reduce the loss of oleic acid vapor to the walls, the loss being otherwise unacceptably high. The solvent was removed in a diffusion dryer and the aerosol subjected to bipolar charging by a Kr-85 radioactive source. Particles of the desired size were selected by an electrostatic classifier (TSI 3071), passed through an aerosol neutralizer (TSI 3054) and transported to a manifold for the impactor calibration. A parallel filter sample was taken to obtain the total mass sampled. The aerosol was continuously monitored by an electrical aerosol analyzer (EAA, TSI 3030) and a laser optical counter (LAC 226, Royco).

The volumetric concentrations of the solution used for different ranges of particle size are given in Table 11. The size distribution detected by the EAA frequently fell within one channel, indicating no detectable fraction of doublets. The average experimental run lasted 30 min. Wall losses in the entire impactor averaged 8.1% or 1% per stage, assuming uniform losses. Because the loss is small and the correction for each stage uncertain, it has been subtracted in the efficiency calculation. The efficiency for stage n was calculated from:

$$E_n = M_n \,/\, \left(M_T\,(1 - W) - \sum_{n+1}^{8} M_i\right) \qquad (5)$$

where M_T is the total mass on the parallel filter and W the fractional wall loss. For particles greater than 0.2 µm, equations (4) and (5) yielded the same efficiency within 5%, showing that these particles do not penetrate the entire impactor.

The aerodynamic particle diameter D_a was obtained by iterating:

$$D_a = D_p \sqrt{\rho_p C(D_p) \,/\, C(D_a)} \qquad (6)$$

with

$$C(D) = 1 + 2\left(6.32 + 2.01 \exp\left(-0.1095PD\right)\right) / 2 \qquad (7)$$

where C is the Cunningham slip factor (17), P is the stage pressure in cm Hg, D_p is the physical diameter in µm determined by the classifier and ρ_p is the particle density in g/cm^3. A value of 1.327 was used for the particle density

assuming that after condensation the particle is still 5% oleic acid. The maximum error in D_a if the particle were pure ammonium fluorescein with a density of 1.35 would be only 0.9%.

As a check that the oil coated particles did not rebound from the stages, some measurements were made with Vaseline particles which should be perfectly sticky. The Vaseline was dissolved in toluene and the mixture from the atomizer was vaporized in the tube furnace. In this case the condensation took place on the very small residue nuclei. The result is a monodisperse aerosol (σ_g = 1.2), so the electrostatic classifier was not used. Therefore the Vaseline measurements also check the electrostatic classifier data. Because the Vaseline aerosol size range from the atomizer is narrowed by the evaporation-condensation process, only the size range from 0.15 to 0.21 µm could be covered with this setup. The Vaseline deposits were weighed to determine stage efficiencies.

The stage efficiencies are plotted against aerodynamic diameter in Figure 8. The efficiency curves for stages 1-4 are not as sharp as those for the upper stages but are still quite satisfactory for sampling purposes. The good consistency between the Vaseline and ammonium fluorescein-oleic acid data confirm the validity of the techniques. Additionally, the deposition spots were well-defined even under high loadings, indicating the absence of bounce.

Comparison of the measured to theoretical 50% cutoff diameters (Table 10) shows agreement for stage 2, but the 50% cutoff diameters for stages 1, 2 and 4 average 27% deviation from theory. The nozzle diameters were measured by microscopy and found to be 0.257 $\pm$ 0.005, 0.43 $\pm$ 0.01 and 0.513 $\pm$ 0.004 mm respectively, within a few percent of the specifications. No pressure taps were available to check the stage pressures. The theoretical predictions are based on incompressible flow, so a deviation from that condition could cause a discrepancy. According to Flagan (18) the cutoff is close to incompressible flow calculations provided that the pressure ratio is greater than 0.5. Overall, we do not regard the disagreement with theory to be serious.

Discussion of the Stage Efficiency Curves

The shapes of the efficiency curves can be compared by plotting the efficiency against the particle diameter normalized by the 50% cutoff diameter (Figure

10). By using the Cunningham slip correction factor in the normalization, we can include the low pressure stages, this normalized aerodynamic diameter being the same as the square root of the normalized Stokes number. Marple's theoretical results (13) based on incompressible flow calculations are drawn as curves in Figure 10 for Reynolds numbers of 3,000, 100 and 10. The jet Reynolds numbers of the Berner impactor range from 1,100 to 1,200 on the upper stages and 1,300 to 3,900 on the lower stages.

It may be worth remarking that the inclusion of the Cunningham slip factor in the efficiency plots significantly improves the match of the curves for the lower stages to those of the upper stages. In other words, the less steep slopes of the curves for the lower stages, evident in Figure 8, are due mainly to the slip factor.

For efficiencies less that 50%, the theory predicts a sharp decrease in efficiency with particle diameter; however, both the upper and lower stages show a small particle tail. Recently Rader and Marple (14) have refined the theory by using a finer grid size for the numerical calculations and by including non-Stokesian drag and interception. The inclusion of interception resulted in a small tail at the low efficiency end. This tail is not pronounced enough to account for the present results but the theory assumed a smooth surface. It is conceivable that the interception effect would increase significantly when the microscopic roughness of the experimental substrate is considered. This suggestion is supported by the observation of a halo extending over several diameters around the central deposition spot. This halo is not caused by particle bounce, but might be formed by particles on an escape trajectory which are captured by surface roughness.. Another possible mechanism of the tail is the observed deposition in the stagnation zone between nozzles, which although small, represents the capture of particles which would not have impacted otherwise.

For efficiencies greater than 50%, the experimental results for the upper stages agree fairly well with the theoretical curve for Re = 3,000. For the lower stages the results are more scattered and the trend closer to the theoretical curves of lower Reynolds number. It is believed that the cause of the sharper curve at high Reynolds number is the flatter velocity profile across the nozzle exit. Since the Reynolds numbers for the lower stages are well above 1,000,

the observed flatter curves must be due to a different effect. Among the unknown influences on the flow field are the non-ideal nozzle entrance and compression effects.

Sampling of Liquid Aerosol

As mentioned above, anomalous effects were observed on stages 1 and 2 in preliminary experiments with liquid particles. This was further investigated with oleic acid aerosol tagged with 1% ammonium fluorescein. Particles in the size range 0.1 to 0.2 μm were generated and calibration experiments carried out with the same techniques previously used. Figure 11 compares the stage collections of 0.14 and 0.17 μm mean diameter oleic acid particles with those for oil-coated ammonium fluorescein. The wall loss, W, is again the difference between the parallel filter catch and the total impactor stage deposits. It therefore possibly includes particles escaping in the impactor exhaust, although this appears unlikely from other evidence.

Figure 11 shows that the loss, W, increased dramatically for oleic acid particles, reaching about 40%. The loss occurs mainly from stage 2 where the peak should be. These particles are not transferred to stage 1, in fact, losses also occur from stage 1. This indicates that the losses are probably not due to shattering of the liquid drops upon impact. Visual examination showed streaking of the oleic acid deposits away from the impaction spots radially inward towards the hole in the center of the stage. Some liquid was observed to have travelled to the edge of the Tedlar foil and then under the foil. Therefore, we conclude that the losses result from the forces produced by the high jet velocities on stages 1 and 2; the deposits are blown away from the foil and lost to the "wall".

These results indicate that impactor data for liquid particles on stages 1 and 2 should be interpreted with reservations. The blowing of liquid away from the impaction spot should be reduced in the presence of solid particles. Indeed, examination of the deposits on stages 1 and 2 from sampling in ambient air does not reveal any evidence of liquid flow.

Particle Bounce and Greased Substrates

Solid particles generated from pure ammonium fluorescein are very bouncy. When these are sampled by the Berner impactor, visual examination of the deposition patterns shows striking evidence of particle bounce. When sticky aerosol is sampled, there is a well-defined round spot under each nozzle and a slight trace of a line between adjacent nozzles corresponding to the stagnation zone. With ammonium fluorescein on a bare plastic substrate, no deposition spot is seen and the lines between nozzles are considerably thicker. The same phenomena occur on the submicron stages; therefore, it cannot be assumed that submicron particles will not bounce.

A common remedy for particle bounce in impactors is to coat the substrate with grease. For sampling acidic particles in ambient air, we require a grease which will suppress bounce but is also compatible with the chemical analysis of the deposit. In particular, a low acid blank is required. Halocarbon grease was found to have the required chemical purity. It was applied to the Tedlar foils by dipping them in a 2% solution of Halocarbon grease in Freon 113. This grease coating was tested for bounce using monodisperse ammonium fluorescein particles of 3 μm aerodynamic diameter. For comparison, the test included uncoated Tedlar foil and Tedlar foil coated with Vaseline, known to be effective in suppressing bounce.

The aerosol generation procedure was the same as during the calibration of the upper stages. The three surface types were exposed to the same amount of aerosol within 5% as determined by the optical counter. The deposits were extracted in 20 mL of ammonium hydroxide and 5 mL of benzene in an ultrasonic bath for one hour. The grease and fluorescein were separated by centrifuging for 15 minutes and the bottom layer containing the fluorescein quantitated in a fluorometer. Blank samples of each of the three surface types were spiked with a known amount of ammonium fluorescein solution and analyzed by the same procedure. The variation between the three blank samples was less than 1%; however, all three were low by 7.8%. It was concluded that the presence of the greases did not affect the analysis; however, the benzene decreased the fluorescence. This did not affect the results which are based on relative amounts.

The distributions of the deposits by stage for the three surfaces and also for liquid aerosol are shown in Figure 12. The distributions for the three surfaces are quite similar indicating that bounce took place from the greased surfaces as well as the ungreased surface. The bounce from the greased surfaces occured because the loadings were relatively high so that the greases became coated with particles and lost some of their ability to suppress bounce. The similarity of the distributions results from the fact that if a particle bounces from one stage, it will probably bounce from succeeding stages also since the jet velocities are even higher. Therefore, bouncing particles are likely either to travel through the impactor or be lost to the wall somewhere. Figure 12 does not reflect the losses but only the relative amounts on each stage.

To assess the losses, we normalize each distribution to the total mass collected when the impactor was loaded with Vaseline substrates. The normalized distributions are plotted in Figure 13. Only 41% of the total mass stays on the ungreased stages while 89% stays on the Halocarbon greased stages. Therefore, Halocarbon is not quite as effective as Vaseline but should be acceptable for ambient sampling. Vaseline is not acceptable because its oily fraction makes aqueous extraction of the deposit more difficult.

The Effect of Relative Humidity on the Sizing of Ammonium Sulfate Aerosol

When the air expands from the high velocity jets in the lower stages the temperature drops, raising the possibility that water vapor might condense on the particles. If the particles gained sufficient mass, they would deposit on an earlier stage than otherwise. Recently, Biswas, et al. (19) reported a significant distortion of a size distribution measured with the Hering impactor at high relative humidity (RH). At our request, Biswas applied his computer calculation to the Berner impactor and predicted a possible growth of particle diameter of 50% at 70% RH. We have therefore conducted an experiment involving the sampling of ammonium sulfate at various relative humidities to look for possible particle growth. Ammonium sulfate was chosen because it is an aerosol of interest and is hygroscopic.

The ammonium sulfate collected on each stage was extracted with water and quantitated with an ion selective electrode. The ammonium probe has a relatively

high detection limit (0.2 ppm) which implied the need for a high aerosol concentration. It was necessary to eliminate the evaporation-condensation process (Figure 9) preceeding the electrostatic classifier. As a result the aerosol was not as monodisperse as during the calibration experiments, the main peak being spread over several channels of the laser counter. The mean diameter was within $\pm$ 5% of that specified by the classifier. The EAA was used only occasionally because of its high flow requirement (50 L/min) and because high humidities caused electrical problems.

The choice of a particle size of 0.17 µm, physical diameter, was a compromise between the increased effect of RH with smaller particles, the need for adequate mass for detection and the laser counter's lower limit of 0.1 µm. The error in mass measurements is estimated to be $\pm$ 5%. The predicted mass fraction on the stages under no growth conditions (Figure 14a) was obtained from the number size distribution of the laser counter and the previously measured efficiency curves. A calculation by Biswas (personal communication) at RH = 70% indicated an increase in particle diameter of about 50% for stages 1-3 and no change for stage 4 and above. As shown in Figure 14b, growth would cause a shift of about 20% of the particles from stage 2 to stage 3. The experimental results for RH = 69% are shown in Figure 14c. The similarity between Figure 14a and 14c implies that no significant particle growth occurs in the Berner impactor.

Earlier experimental work by Hochrainer and Zebel (20) did not find any detectable change in particle size with humidity in a Mercer cascade impactor. The explanation for why the theoretically predicted growth did not occur involves the short residence time in the jet. For stages 1-3, the time is less than 10 µsec. When the jet expands the air supersaturates, but before condensation can take place, the jet is recompressed on the stage and the temperature rises. Hochrainer and Zebel reached a similar conclusion.

Bounce of Ammonium Sulfate Particles

The effect of RH on the bounce of ammonium sulfate particles was observed on 0.23 µm particles at three different RH's. The results are shown in Figure 15. To examine the magnitude of wall loss, which is a good indicator of particle

bounce, the collected mass on each stage is normalized by the total sampling mass for the parallel filter. The wall loss reduces from 36% at 28% RH to 3% at 77% RH. Rebound from stage 3 at RH = 28% is evident. Otherwise the size distributions are similar. Again, there is no evidence of particle growth.

The wall loss was also investigated with polydisperse aerosol with number mean diameter of 0.22 μm, generated by the same system without the classifier, which increased the aerosol concentration by an order of magnitude. The percentage of mass collected on the stages for both monodisperse and polydisperse aerosol is plotted in Figure 16 vs RH. The collected mass fraction increases linearly with RH, passing 90% at about 60% RH. Therefore, above this RH, ammonium sulfate could be sampled from the atmosphere with ungreased substrates.

Greased substrates are normally required for ambient sampling. It is necessary to know the maximum loading before the grease becomes ineffective in preventing particle bounce. The polydisperse 0.22 μm ammonium sulfate aerosol was used to study loading on Vaseline. Table 12 lists the fraction of the mass retained on the stages for increasing mass sampled. A loss of 10% occurs at a total loading of about 600 μg. Since 90% of the mass was on stages 3 and 4, the loading per stage was about 300 μg. During previous 40 hour sampling in Los Angeles (2,4), the maximum loading obtained was about 130 μg of ammonium sulfate on stage 4 and less than 50 μg on all other stages. Therefore, the capacity of the grease is generally adequate to prevent bounce under field conditions.

Evaporation Loss of Ammonium Nitrate

Another question concerning impactor performance is what is the extent of evaporative loss when a volatile material is sampled? The reduced pressure on the lower stages might be expected to accelerate the loss. To study this question, we used ammonium nitrate particles, an important pollutant, with large volatilization losses during filter sampling.

Polydisperse ammonium nitrate aerosol was generated with a mass median diameter of 0.16 μm. The impactor was operated for a preselected time to

collect ammonium nitrate particles on greased Tedlar foils. Then the loaded foils were carefully cut along a diameter into two equal pieces. One half was removed as a reference and the other half kept in the impactor. Dry, clean air was drawn through the impactor for a timed period. The ammonium nitrate remaining on the halved substrate was then quantitated by selective ion electrode for ammonium ion and the difference from the reference half gave the evaporative loss. The errors in this procedure were sizeable. Measurements made after the cutting but with no additional exposure showed $\pm$ 8.7% variation between the two halves, reflecting a non-uniformity in the sampling on the two sides of the impactor. Some misalignment of the jets to the deposition spots could occur during the reassembly of the stages in spite of considerable care.

Dry air at less than 20% RH was used in the experiments. Since the dissociation constant of ammonium nitrate does not vary with RH below the deliquescence point, the precise value of the RH is unimportant. Preliminary experiments at room temperature for 64.5 hours gave an average loss of 12%. Because of the large uncertainties, meaningful values could not be obtained for individual stages.

Parallel filter samples were taken to obtain a comparison of the evaporative losses with those in the impactor. Two 47 mm Teflon membrane filters (2 µm Zefluor) were loaded simultaneously, one backed by a Nylon membrane filter (21) to collect the nitric acid from the evaporated nitrate. After drawing dry clean air through the filters for a predetermined time, the nitrate on each filter was measured by ion chromatography. Analyses of ammonium ion on the two Teflon filters by specific ion electrode agreed with the nitrate determination within 3%. The two Teflon filters were found to be equally loaded, within 3.5%. Room temperature experiments with 7 hour exposures showed a 40% loss from the Teflon filters.

To investigate an extreme case of high temperature and low RH (but not unrealistic for California), additional measurements were made in a room-sized environmental chamber at 35 $\pm$ 0.5^{o}C (95^{o}F) and RH = 18 $\pm$ 2%. The entire apparatus was inside the chamber so that all internal surfaces were temperature equilibrated, a more realistic test than merely sampling heated air. Losses were determined for 6, 12 and 24 hours exposures. The results are listed in Table

13. The impactor data are averages over stages 1-6. The losses in the impactor of up to 7% are acceptable for field sampling while the 81-95% losses from the filter are not.

The striking difference between the losses from the impactor and the filter is at first surprising but there is a reasonable explanation in terms of the difference in boundary layers and the geometry of the deposits. The boundary layer will be thicker in the stagnation zone of the impactor surface (where the deposition spot is located) than on the filter where the air flow surrounds filter elements of the order of 10 μm diameter. The mass transfer will be slower in the boundary layer where molecular diffusion is the transport mechanism.

However, we believe the main reason for the difference is the much larger exposed surface area per unit mass of the deposits on the filter. In the impactor, the particles pileup in a spot. Evaporation will occur from the outer layer of particles but those covered up will be protected. This mechanism implies that the evaporative loss should decrease with areal loading. . That this is the case is shown by Figure 17. The figure includes additional runs to explore the loading effect. Absolute values of the areal loadings should be disregarded since it is impossible to calculate the exposed area of the deposits. However, relative values for the filter or impactor, i.e., the slopes of the lines are accurate. The evaporative loss decreases somewhat faster than inversely with loading and even faster at higher flow rate. These data clearly demonstrate the importance of exposed surface area. Thus the impactor has a strong advantage over a filter as a collector of volatile materials.

Size Distribution of Acidic Species in Oildale and Berkeley

Impactor Substrates and Chemical Extractions

Fluorocarbon foils (Tedlar) were used as collection media on all impactor stages, but a fluorocarbon grease coating was added (Halocarbon #25-5S) to inhibit particle bounce. For sampling at Oildale only the first 3 stages were greased by wiping to produce a thin film. Berkeley sampling utilized thinner more uniform grease coatings on all stages applied by dipping the foils in a 2% solution with highly volatile Freon 113 as the solvent. Laboratory testing indicated

Halocarbon #25-5S to be as effective as a hydrocarbon grease, Apiezon L, commonly used for bounce reduction. Unlike Apiezon, Halocarbon grease is chemically inert even to strong mineral acids. Stage 9, which serves only to prevent coarse particles from entering the impactor, was heavily greased.

Impactor samples were stored under dry ice to inhibit post-sampling chemical reactivity until water-extracted for analysis. The extraction and analysis procedure has been described previously (2,4). Less than detectable levels of the ions analyzed were extracted from either coated or uncoated Tedlar foil blanks. A small consistent nitrate blank (4.5 μg/foil), corrected for in the Berkeley sample sets, was traced to a specific batch of factory-sealed polypropylene extraction tubes.

Extraction recovery was assessed by reextracting the previously analyzed atmospheric samples for comparison. The same aqueous extraction procedure was repeated on bare foils, while coated foils were reextracted first in Freon to dissolve the grease and then back-extracted into the aqueous phase for analysis. For both greased and ungreased foils the single aqueous extraction efficiency was > 95% for all ionic species, with the second extraction leaching less than detectable amounts in many cases.

Ambient Size Distributions

The distributions by impactor stage were combined with the measured stage efficiencies and analyzed by an inversion routine (22) to obtain particle size distributions. The results are plotted in Figures 18-23.

The Oildale sampling site and atmospheric conditions have been described previously. In Berkeley, the impactor was located on the roof of the eight story Department of Health Services building in downtown Berkeley with the inlet 1.7 m above roof level. The first two sampling periods at Berkeley were characterized by poor visibility with polllutant build up under a growing inversion layer. The period October 2-5 included especially hot dry days with large scale visibility reduction. The last two Berkeley sampling periods were relatively clean with reestablishment of the normal marine air circulation patterns.

Large particle nitrate was observed at both Berkeley and Oildale but was predominant only during well ventilated periods of high visibility. Visibility reduction was associated with fine particle nitrate. At Berkeley the bimodal distribution merged during the period of highest visibility reduction to include particles 1-2 μm (Stage 5) with good light scattering potential. At Berkeley during clean marine ventilated regimes, large particle nitrate occurs with Na and Cl from sea salt. With low visibility Cl is suppressed and NO_3 occurs with Na primarily. At Oildale large particle nitrate is associated with ammonium perhaps due to windblown fertilizer.

The highly correlated size distributions for sulfate and ammonium at Berkeley, and to a lesser degree at Oildale, suggests the presence of ammonium sulfate salts as observed before in the L.A. air basin. At Oildale the sum of sulfate and nitrate appear to be better correlated with ammonium than sulfate alone.

The fine particulate mode in Oildale distributions (Figures 18 and 19) peak at smaller particle size than in the Berkeley distributions (Figures 20-23). This might be due to the lower humidity at Oildale. However, since the Oildale sampling was done with grease on the upper three impactor stages only, particle bounce could have contributed to the observed effect.

Significantly smaller levels of free strong acid were estimated to have been present in Berkeley than in Oildale or the L.A. air basin. Total acid levels as the sum of the impactor stages at Berkeley was near 0.5 $\mu g/m^3$ (as H_2SO_4) except for the period of highest visibility reduction when it reached 0.9 $\mu g/m^3$. Levels at Oildale were 0.9 $\mu g/m^3$, compared to concentrations which exceeded 1.4 $\mu g/m^3$ in the central L.A. air basin. In all cases strong acid peaked on stage 3 or 4 exhibiting shifts to smaller size during hot dry periods.

IV. Summary and Conclusions

This report covers Phase III of a research program to make baseline measurements of dry acid deposition in California, to develop measurement techniques for dry deposition and to study the mechanisms of dry deposition.

A bubbler with high sensitivity for sulfur dioxide was further tested under extreme conditions of high temperature and low humidity at Oildale. After the solution volume was increased, the bubbler performed well for 10 consecutive weeks.

The deposition of particulate sulfate and nitrate on leaves and surrogate surfaces was measured directly by washing off the deposits. Deposition velocities on leaves were found to be independent of exposure times ranging from 14 to 62 days under nearly unvarying meteorological conditions. Exposures of 6 or 7 days sometimes gave higher deposition velocities for unknown reasons. The deposition velocities were found to be approximately the same for all the surfaces, natural and surrogate. The studies included pine needles in adddition to broad leaves. Surrogate surfaces had detectable deposits only on the top surface. Deposition velocities for nitrate were 30 to 40% larger than for sulfate, attributable to the larger sizes of nitrate particles. Oildale deposition velocities were generally larger than those found previously in Western Los Angeles and Tanbark Flats.

Experimental work was conducted on a Nuclepore surrogate "leaf" as a passive sampler for sulfur dioxide which can be placed in a canopy. In Oildale it was necessary to shield the "leaves" from direct sunlight to prevent drying. The Nuclepore "leaf" sampled SO_2 and NO_x at a relative rate consistent with the bubbler; however, the measured rate was much higher than calculated from diffusion theory, probably because of wetting of internal surfaces.

An extensive study was made of the Berner cascade impactor in order to establish a reliable method for the measurement of the size distributions of acidic particles. The stage efficiencies were calibrated with monodisperse laboratory aerosols, which required considerable development work for the submicron aerosols. The stage cutoffs were found to be sharp, the upper stage cutoffs being in excellent agreement with theory and the lower stages in moderately good agreement. Wall losses are small. Liquid oleic acid was found to undergo blowoff from the last two stages. However, this effect was not seen for ambient sampling. Solid particles, even submicron, were seen to bounce from uncoated substrates. Halocarbon grease, which is compatible with acid analyses, was shown to suppress bounce effectively. The performance of the Berner impactor for two of the principal ambient particle pollutants, ammonium sulfate and ammonium nitrate,

was also studied in the laboratory. Ammonium sulfate particles were found to be sized correctly even at high relative humidity, ruling out the possibility that, under high jet expansions, a significant amount of water might condense on the particles. This result was attributed to the extremely short time the particles spend in the expanding jet. High relative humidity was observed to suppress the bouncing of ammonium sulfate particles. The capacity of a greased surface to suppress the bouncing of dry ammonium sulfate particles was determined to be adequate under loadings representative of ambient sampling.

Losses of ammonium nitrate from volatilization in the Berner impactor were observed to range from 3 to 7% at 35°C and 18% R.H. Filter losses were 81-95% under the same conditions. This result is explained in terms of the exposed surface area per mass of deposit. Measurements showed the evaporative loss to decrease somewhat faster than inversely with loading. Thus the Berner impactor is a good sampler for ammonium nitrate.

Particle size distributions were measured in Oildale and Berkeley with the Berner impactor. The deposits were analyzed for strong acid, sulfate, nitrate, ammonium, sodium and chloride ions. The sulfate and ammonium are in the same submicron mode but the nitrate is bimodal. The relative amounts of fine and coarse nitrate are different for clean and polluted conditions. Strong acid was in the fine fraction.

In summary, the Berner impactor was thoroughly tested in the laboratory and in the field. It was shown to sample ammonium sulfate and ammonium nitrate without artifacts. Data were obtained on the ambient size distributions of the major acidic ions. Thus a technique has been proven for measurement of the size distributions of acidic particles in California.

V. Recommendations

(1) The hydrogen peroxide bubbler has been shown to be a reliable sampler for sulfur dioxide with sufficient sensitivity for dry deposition. It should be deployed in networks since the electronic monitors currently in use lack adequate sensitivity.

(2) Leaf washing yields reproducible results for nitrate and sulfate deposition. The technique has also been demonstrated for pine needles. This affords a direct measurement of deposition on leaves and needles without the uncertainties attending other methods. Large areas of California are forested; these vulnerable targets for acid impact should be studied by the leaf washing technique.

(3) Dry deposition of acidic particles depends strongly on particle size. In this work, the Berner impactor was proven to be an excellent sampler for acidic particles; no other sampler has been so validated. Future studies of air quality in California should include particle size measurements using the techniques developed in the present work.

VI. Acknowledgements

We thank the staff of the Aerometric Data Division for permission to locate our sampling experiment at the ARB monitoring station in Oildale and the cooperation of Debra Wright, station operator. We also appreciate the assistance of Jeff Cook in obtaining the ARB data tape.

We thank Dr. Axel Berner for the loan of his impactor and for helpful discussions. Dr. Evaldo Kothny made the acid titrations. We appreciate the continuing interest and support of our ARB contract manager, Dr. Praveen Amar.

VII. References

1. John, W., Wall, S.M. and Wesolowski, J.J.: Assessment of dry acid deposition in California. Final Report, Interagency Agreement (ARB No. A1-053-32), Air and Industrial Hygiene Laboratory Report CA/DOH/AIHL/SP-31, California Department of Health Services, June 1984.

2. John, W., Wall, S.M. and Ondo, J.L.: Dry Acid Deposition on Materials and Vegetation: Concentrations in Ambient Air. Final Report, Interagency Agreement (ARB No. A1-160-32), Air and Industrial Hygiene Laboratory Report CA/DOH/AIHL/SP-34), California Department of Health Services, May, 1985. Available from NTIS, Report No. PB85-241206/WEP.

3. John, W., Wall, S.M., and Ondo, J.L.: Measurements of dry acid deposition in California. 77th Annual Meeting of the Air Pollution Control Association, San Francisco, CA, June 24-29, 1984, Paper No. 84-108.1.

4. Wall, S., Ondo, J.L. and John, W.: Strong acid aerosol size distributions in the Los Angeles Air Basin. Paper No. 84-108.2, ibid.

5. Ondo, J.L., John, W. and Wall, S.M.: Dry acid deposition on leaves of ligustrum and a new surrogate leaf. Paper No. 84-108.3, ibid.

6. Mulik, J., Puchett, R., Williams, D. and Sawicki E.: Ion chromatographic analysis of sulfate and nitrate in ambient aerosols. Anal. Lett. 9(7):653-663, 1976.

7. Mulik, J.D., Todd, G., Estes, E., Puckett, R., Sawicki, E. and Williams, D.: Ion Chromatographic Determination of Atmospheric Sulfur Dioxide. In: Ion Chromatographic Analysis of Environmental Pollutants. E. Sawicki, J.D. Mulik, and E. Wittgenstein, eds., Ann Arbor Science Publisher, Inc. Ann Arbor, MI, 1978. pp. 23-40.

8. Appel, B.R., Tokiwa, Y., Haik, M. and Kothny, E.L.: Artifact Particulate Sulfate and Nitrate Formation of Filter Media. Atmos. Environ. 18:409 (1984).

9. Sehmel, G.A.: Particle and Gas Dry Deposition: A Review. Atmos. Environ. 14:983-1011 (1980).

10. Berner A., Lurzer, C.H., Pohl, L., Preining, O. and Wagner P.: The size distribution of the urban aerosol in Vienna. Sci. of the Total Environ. 13:245-261 (1979).

11. Hering, S.V., Flagan, R.C. and Friedlander, S.K.: Design and Evaluation of a New Low Pressure Impactor I. Environ. Sci. Technol. 12:667 (1978).

12. Fluid Dynamics, Daily, J.W. and Harleman, D.R.F. Addison-Wesely, Reading, MA, 1966.

13. Marple, V.A. and Liu, B.Y.H.: Characteristics of Laminar Jet Impactors. Environ. Sci. Technol. 8:648-654 (1974).

14. Rader, D.J. and Marple, V.A.: Effect of Ultra-Stokesian Drag and Particle Interception on Impaction Chracteristics. Aerosol Sci. Technol. 4:141-156 (1985).

15. Berglund, R.N. and Liu, B.Y.H.: Generation of Monodisperse Aerosol Standards. Environ. Sci. Technol. 7:147-153 (1973).

16. Liu, B.Y.H.: Laboratory Generation of Particulates with Emphasis on Submicron Aerosols. J. Air Pollut. Control Assoc. 24, No. 12, Dec. 1974.

17. Aerosol Technology, Hinds, W.C. John Wiley & Sons, New York, 1982.

18. Flagan, R.C. J. Colloid Interface Sci. 87:291-299 (1982).

19. Biswas, P., James, C.L. and Flagan, R.C.: Distortion of Size Distributions by Particle Sampling Instruments. In: Aerosols, Liu, Pui and Fissan, eds., Elsevier Sci. Publ. Co., Inc., New York, 1984, p. 191.

20. Hochrainer, D. and Zebel, G. The Influence of the Expansion Humidity on the Deposition of Particles in Impactors. J. Aerosol Sci. 12:49-53 (1981).

21. Appel, B.R., Wall, S.M., Tokiwa, Y. and Haik, M. Simultaneous nitric acid, particulate nitrate and acidity measurements in ambient air. Atmos. Environ. 14:549-554 (1980).

22. Markowski, G.R. (1986). Improving Twomey's algorithm for inversion of aerosol measurement data. Unpublished manuscript.

Table 1

Mean Value and Variation with Measurement Period of Atmospheric Variables

Variable	Mean Value	Units	Std. Dev., %
Sulfate	5.0 ± 0.7	$\mu g/m^3$	13
Nitrate	7.6 ± 1.5	$\mu g/m^3$	25
SO_2 (bubbler)	7.5 ± 0.3	ppb	4
NO (ARB monitor)	12.2 ± 1.0	ppb	12
NO_2 (ARB monitor)	18.0 ± 2.1	ppb	12
NO_x (ARB monitor)	30.2 ± 2.6	ppb	9
THC (ARB monitor)	3.7 ± 0.6	ppm	16
CH_4 (ARB monitor)	3.1 ± 0.7	ppm	23
O_3 (ARB monitor)	51 ± 7	ppb	14
Wind Direction	299 ± 16	deg	-
Wind Speed	6.5 ± 0.5	km/hr	7
Temperature	28 ± 2.7	^oC	10
Relative Humidity	41 ± 3	%	8

Table 2

Comparison of Sulfate and Nitrate Concentrations for Hivol, SSI and Monocut Samplers at Oildale

	Concentrations, $\mu g/m^3$			Ratios	
Sampler:	Hivol	SSI	Monocut	Monocut / SSI	Monocut / Hivol
Period:	9/3/84 - 10/3/84		8/30-10/4		
Sulfate	10.6	5.4	5.5	1.02	0.52
Nitrate	10.0	1.17	1.67	1.43	0.17

Table 3

Measured Deposition Velocities (cm/s) for Sulfate on Various Surfaces

Surface	6-7 Day Exposure	13-62 Day Exposure
L. ovalifolium	0.10 ± 0.04	0.05 ± 0.01
L. japonicum	0.14 ± 0.01	0.13 ± 0.02
P. coulteri	0.15 ± 0.07	0.14 ± 0.03
Tedlar-top	0.12 ± 0.09	0.19 ± 0.10
Tedlar-bottom	< 0.02	< 0.02
Nuclepore "leaves"*		
8 µm-top	0.17 ± 0.09	0.12 ± 0.02
8 µm-bottom	< 0.04	< 0.04
0.03 µm-top	0.13 ± 0.11	0.11 ± 0.02
0.03 µm-bottom	< 0.04	< 0.04
8 µm, peroxide-top	0.18 ± 0.09	0.17 ± 0.16
8 µm, peroxide-bottom	2.1 ± 1.0	2.0 ± 0.5
0.03 µm, peroxide-top	0.14 ± 0.04	0.13 ± 0.08
0.03 µm, peroxide-bottom	0.8 ± 0.8	1.5 ± 0.4

*Top surface Tedlar, bottom surface Nuclepore.

Table 4

Measured Deposition Velocities (cm/s) for Nitrate on Various Surfaces*

Surface	6-7 Day Exposure	13-62 Day Exposure
L. ovalifolium	0.15 ± 0.04	0.07 ± 0.03
L. japonicum	0.33 ± 0.06	0.16 ± 0.03
P. coulteri	0.5 ± 0.2	0.30 ± 0.11
Tedlar-top	0.2 ± 0.1	0.2 ± 0.1
Tedlar-bottom	< 0.02	< 0.02
Nuclepore "leaves"		
8 µm-top	0.2 ± 0.1	0.13 ± 0.08
8 µm-bottom	< 0.02	< 0.02
0.03 µm-top	0.17 ± 0.02	0.13 ± 0.08
0.03 µm-bottom	< 0.02	< 0.02
8 µm, peroxide-top	0.2 ± 0.1	0.2 ± 0.1
8 µm, peroxide-bottom	< 0.04	< 0.04
0.03 µm, peroxide-top	0.2 ± 0.1	0.2 ± 0.1
0.03 µm, peroxide-bottom	< 0.2	< 0.02

*Listed uncertainties are standard deviations of repeated measurements.

Table 5

Ratio of Deposition Velocities on Leaves to those on Surrogate Surfaces*

Surface	Sulfate	Nitrate
L. ovalifolium	0.4	0.4
L. japonicum	1.0	0.9
P. coulteri	2.0	1.0

*For 13-62 day exposures. Averaged over all surrogate surfaces, top only.

Table 6

Comparison of Deposition Velocities (cm/s) Measured at Three Locations

Location	Exposure	Sulfate			Nitrate		
		L. japon.	L. oval.	Surrogate **	L. japon.	L. oval.	Surrogate **
W. Los Angeles	4 days	0.69*	0.64*	0.07	0.24	0.15	0.12
Tanbark Flats	4 days	0.06	0.03	< 0.03	0.10	0.06	0.08
Oildale	6-7 days	0.14	0.10	0.07	0.33	0.15	0.09

*High value attributed to SO_2 deposition.

**Surrogate surfaces averaged over both sides.

Table 7

Internal Deposition Rates of SO_2 and NO_x in Nuclepore "Leaves"

Configuration	Ratio to 8 µm pore, water	
	Sulfate	Nitrate
8 µm pore, water	1 (2.9 ± 0.5 µg/day)	1 (2.2 ± 1.2 µg/day)
0.03 µm + 0.05 µm, water	0.8 ± 0.2	0.7 ± 0.2
8 µm, peroxide	1.9 ± 1.2	1.0 ± 0.3
0.03 µm + 0.05 µm, peroxide	1.2 ± 0.5	1.5 ± 0.5

Table 8

Rate of Water Loss from Nuclepore "Leaves" (8 µm pore)

Location	Temperature Range	RH Range	Measured Water Loss	Measured/Calculated	
				Screen*	Nuclepore**
West Los Angeles	20-30°C	50-90%	3.7 g/day	80	1.3
Tanbark Flats	8-24°C	40-90%	2.0 g/day	54	0.9

*Thickness of screen used as diffusion length.

**Thickness of Nuclepore used as diffusion length. (See Text)

Table 9

Comparison of Measured to Theoretical Rates of Sampling of SO_2 and NO_x by the Nuclepore "Leaves" (8 µm pore)

Location	Measured/Theoretical SO_2	NO_x
West Los Angeles	4.1	2.5
Tanbark Flats	6.6	7.0
Oildale	3.9	5.5
Mean ± S.D.	4.9 ± 1.5	5.0 ± 2.3

Table 10

Stage Parameters of the Berner Impactor

(1) Stage Number	(2) No. of Holes	(3) Hole Dia. (mm)	(4) Pressure Ratio P/P_o	(5) Velocity m/s	(6) Cutoff Dia. (µm) St* = 0.22	(7) Cutoff Dia. St = 0.24	(8) Cutoff Dia. Exp.	(9) Residence Time (µsec)
9	1	16.6	1.000	2.31	16.0	16.7	-	-
8	7	5.5	1.000	3.01	8.0	8.4	8.6	3350
7	13	2.8	1.000	6.25	4.0	4.18	4.2	810
6	26	1.4	0.995	12.5	2.0	2.09	2.1	240
5	50	0.75	0.991	26.0	1.0	1.04	0.96	77
4	30	0.60	0.954	64.0	0.50	0.52	0.43	23
3	22	0.50	0.814	153	0.25	0.26	0.21	9.7
2	30	0.40	0.485	227	0.125	0.13	0.13	4.4
1	130	0.25	0.324	227	0.060	0.063	0.082	3.3

*St ≡ Stokes Number

Table 11

Aerosol Parameters for Lower Stage Calibrations

Solution Concentration %	Median Dia. (µm)	Particle Size Range
0.025	0.05	0.056 - 0.09
0.1	0.08	0.09 - 0.15
0.5	0.14	0.15 - 0.25
2	0.22	0.25 - 0.35
5	0.29	0.35 - 0.43

Table 12

Fraction of Sampled Ammonium Sulfate Retained on Vaseline-coated Substrates vs. Loading

Sampled Mass µg	Fraction of Sampled Mass on Stages, %
154	100
215	100
664	88
1682	81

Table 13

Evaporative Losses of Ammonium Nitrate from Impactor and Filter Samples

Exposure to Air Flow,* Hours	Impactor		Filter	
	Initial Mass per Stage, µg	Mass Loss, %	Initial Mass per Filter,** µg	Mass Loss, %
6	208	3	171	95
12	147	7	252	81
24	93	7	372	87

*30 L/min Flow Rate, 35°C, 18% RH.

**47 mm Dia. Filter

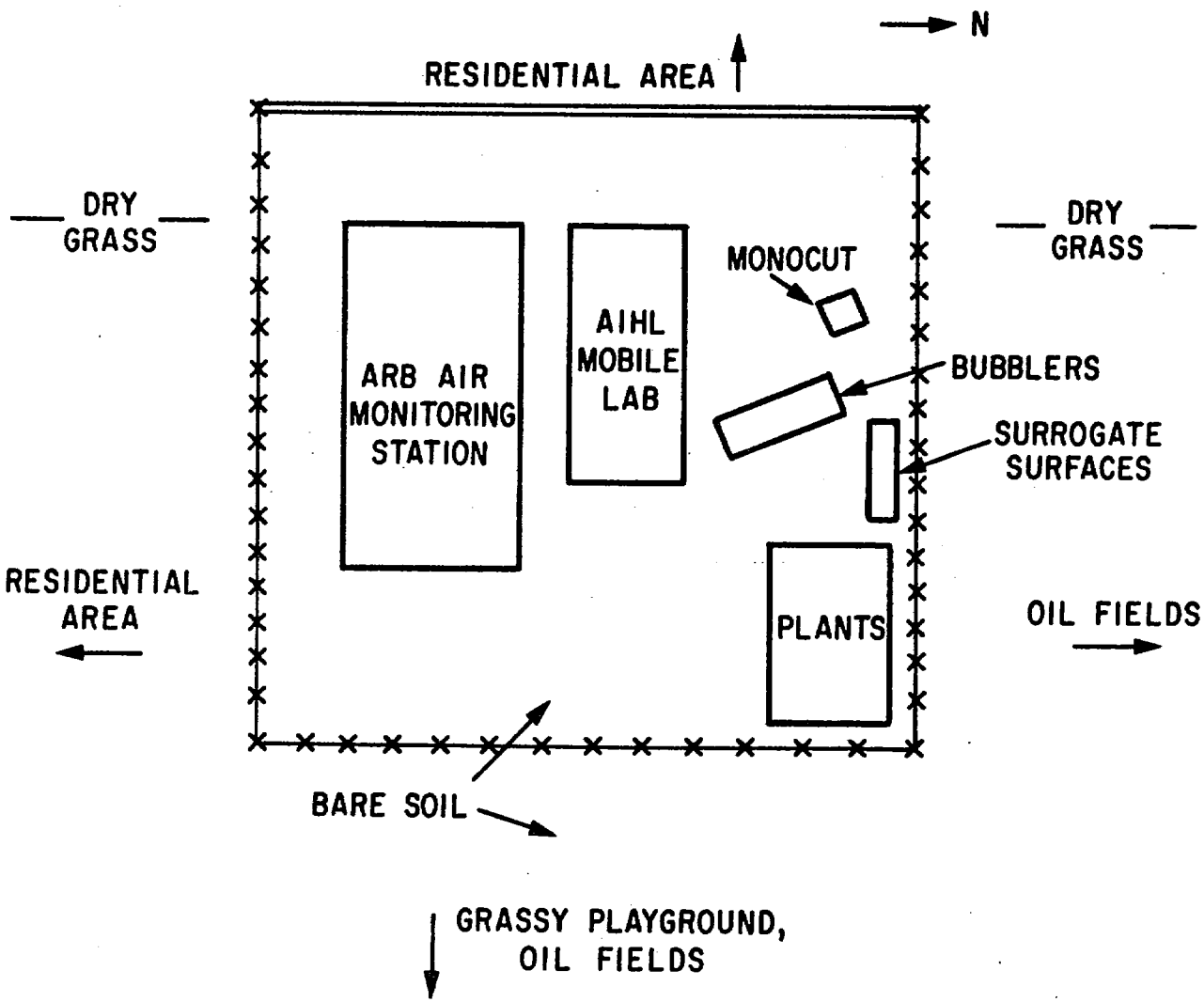

Figure 1. Sampling layout at Oildale.

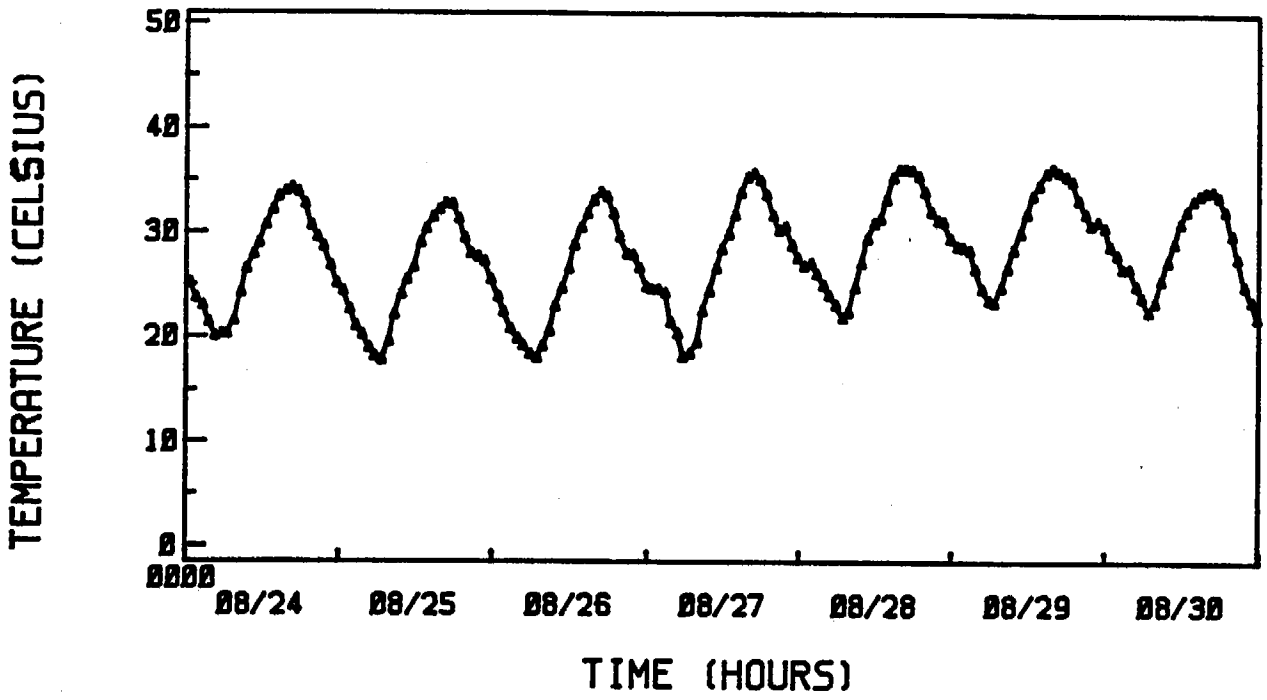

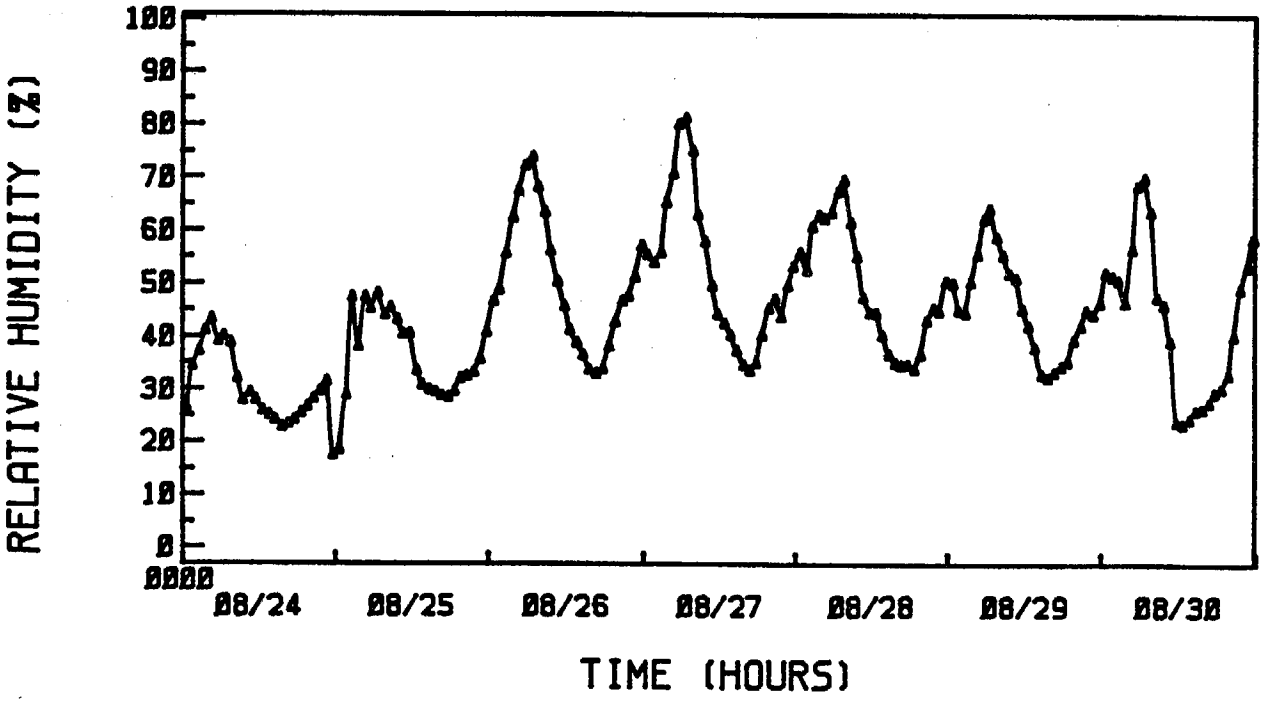

Figure 2. Hourly averages of temperature and relative humidity during a typical week of the study at Oildale.

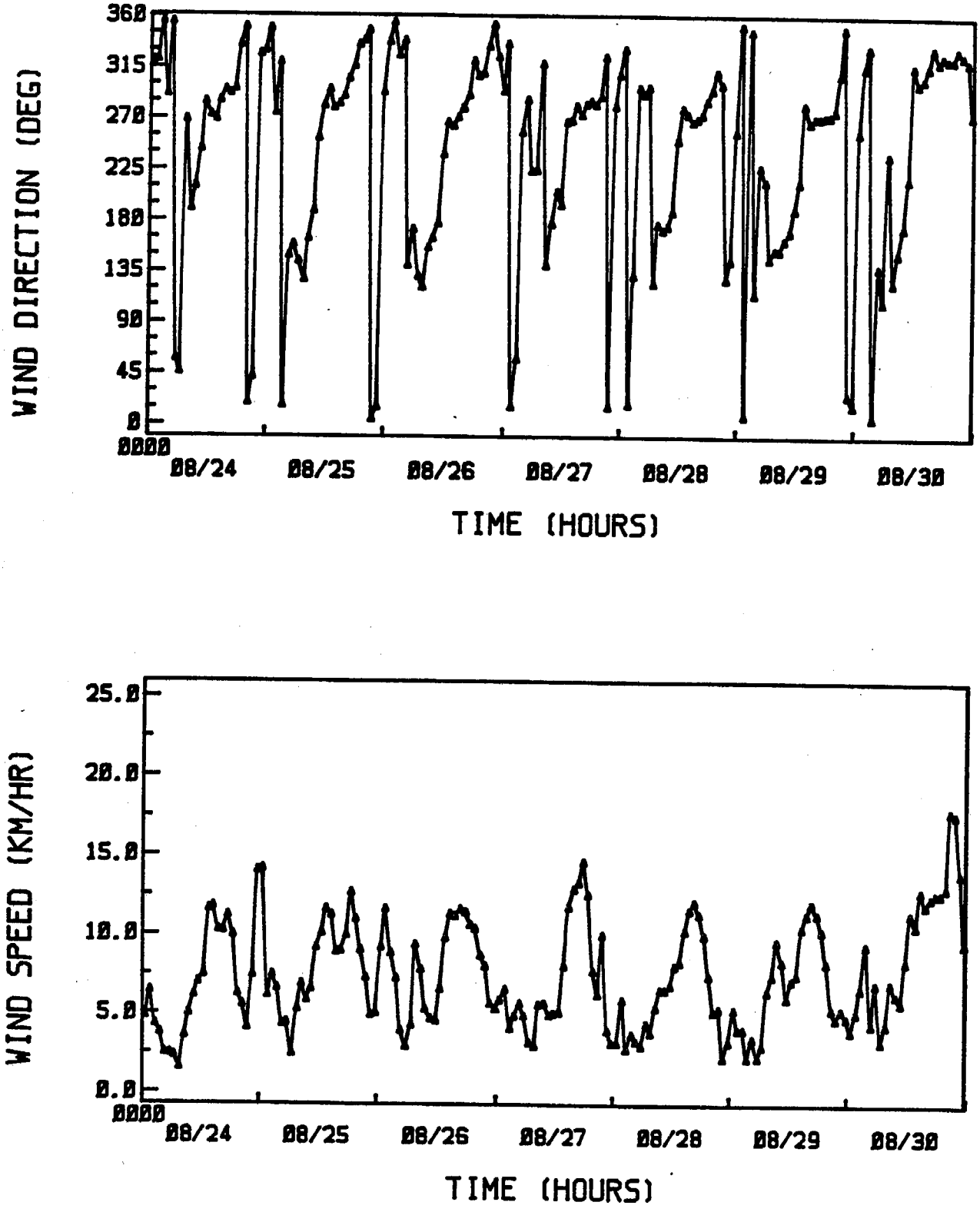

Figure 3. Hourly averages of wind direction and wind speed at Oildale.

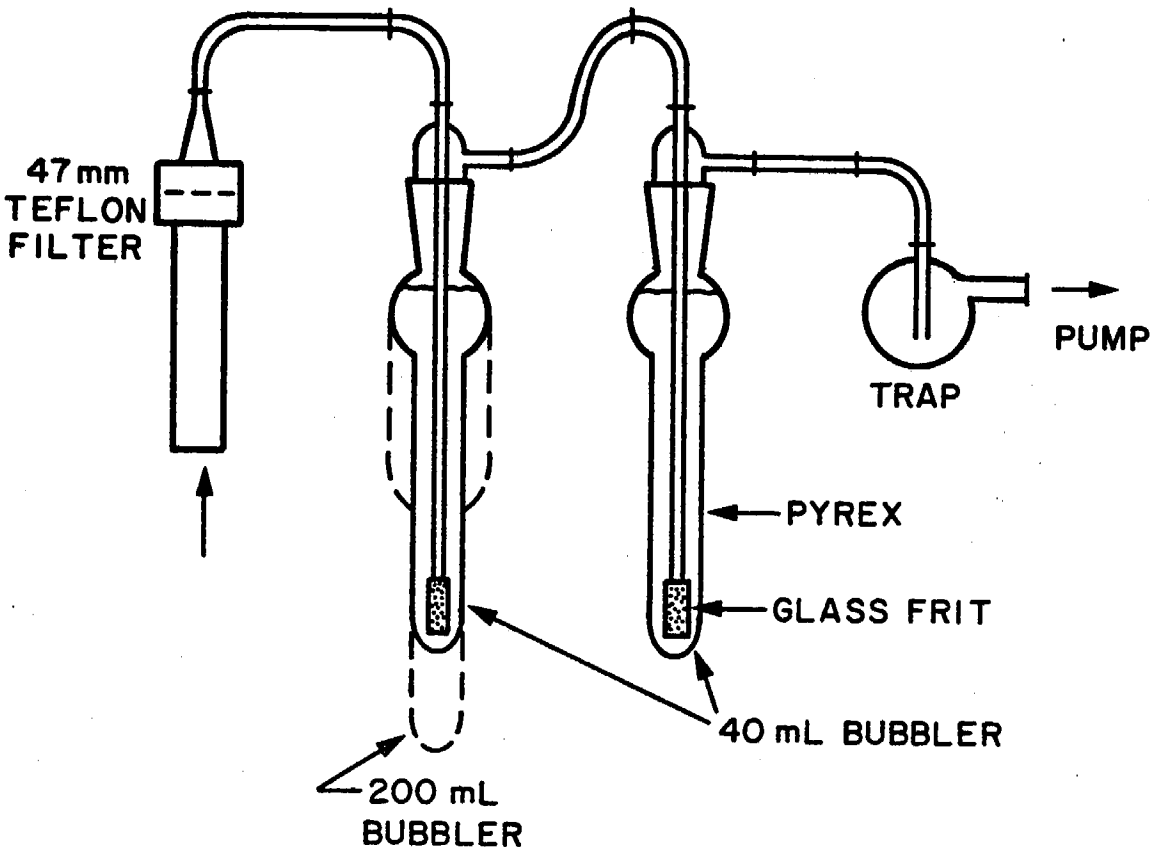

Figure 4. Bubbler for sulfur dioxide sampling.

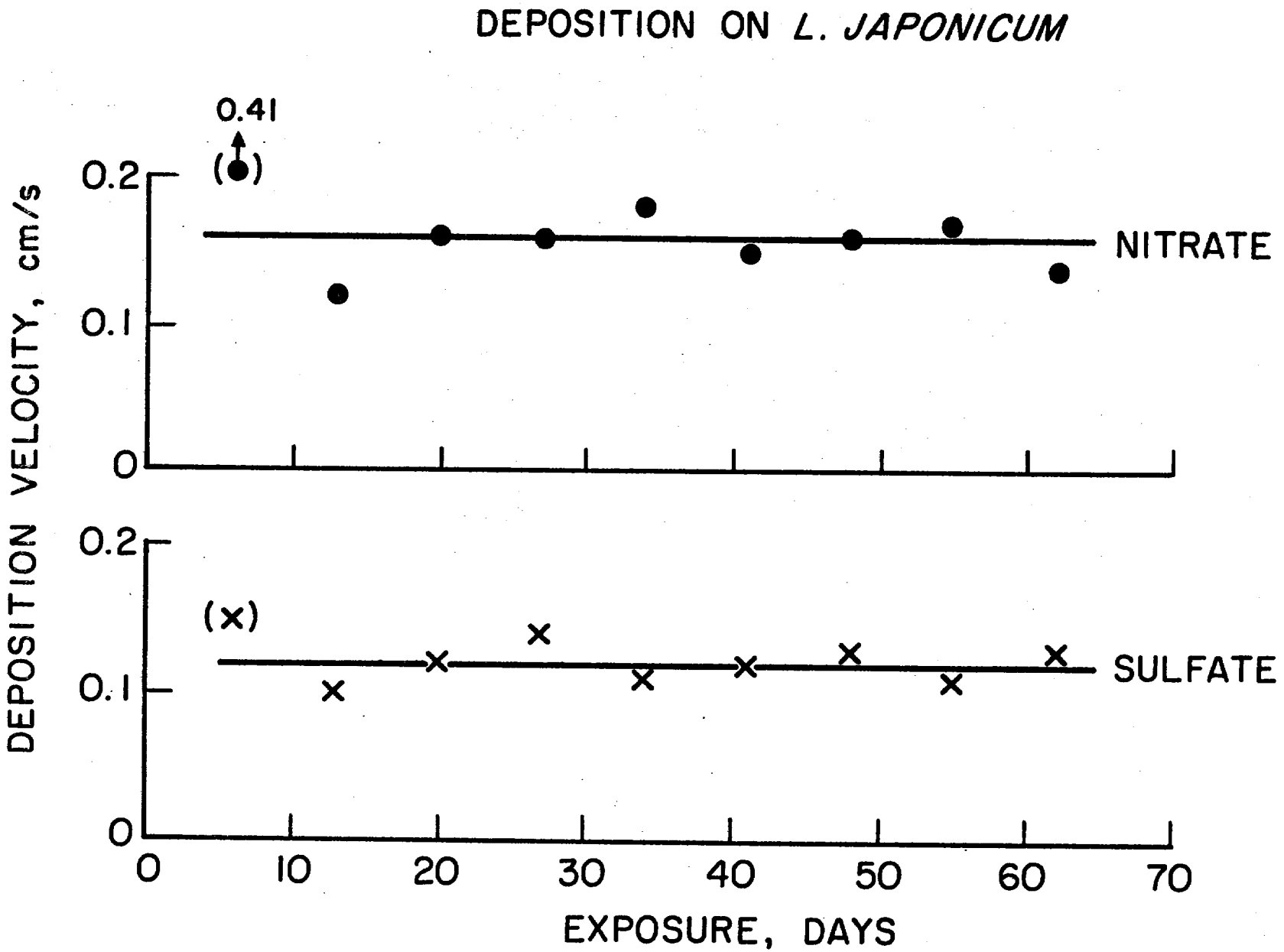

Figure 5. Deposition velocities of sulfate and nitrate on leaves showing independence of exposure period except for the six day data points, which are higher.

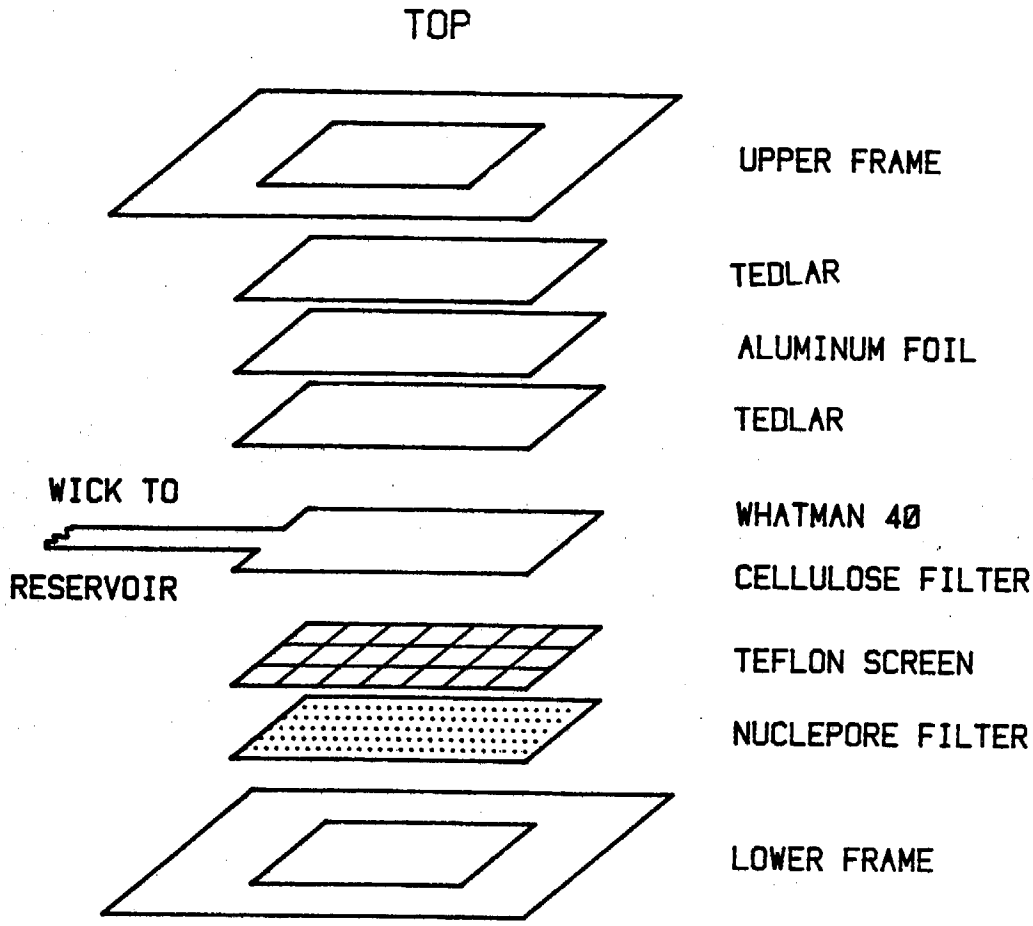

Figure 6 . Construction of Nuclepore surrogate leaf.

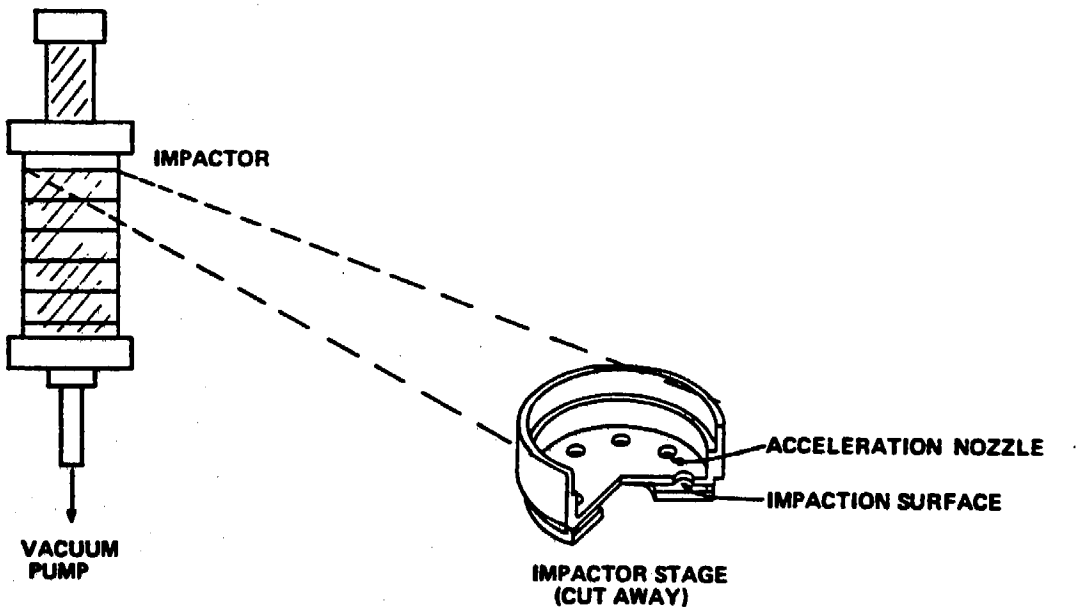

Figure 7. The Berner cascade impactor.

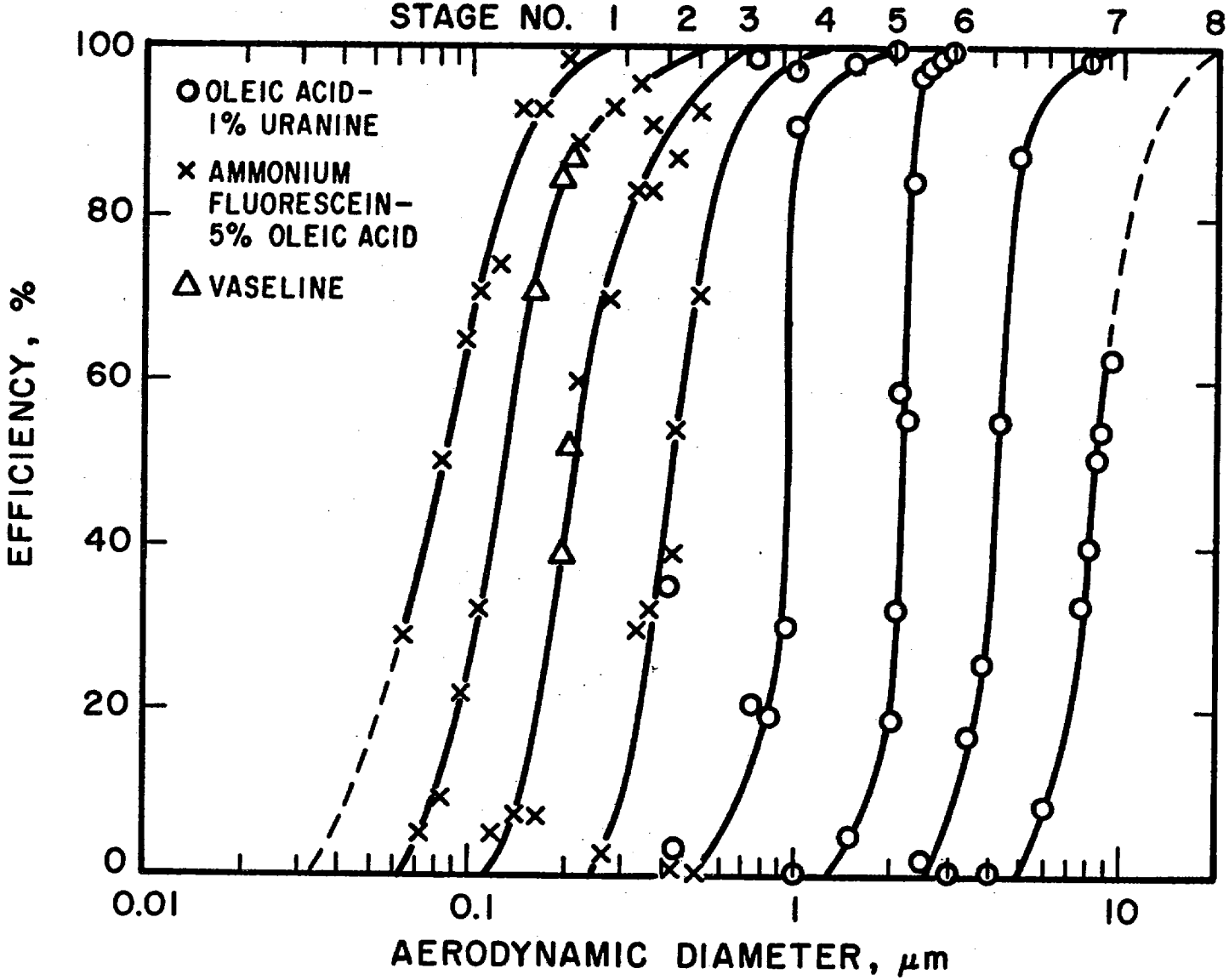

Figure 8. Efficiency curves for the stages of the Berner impactor.

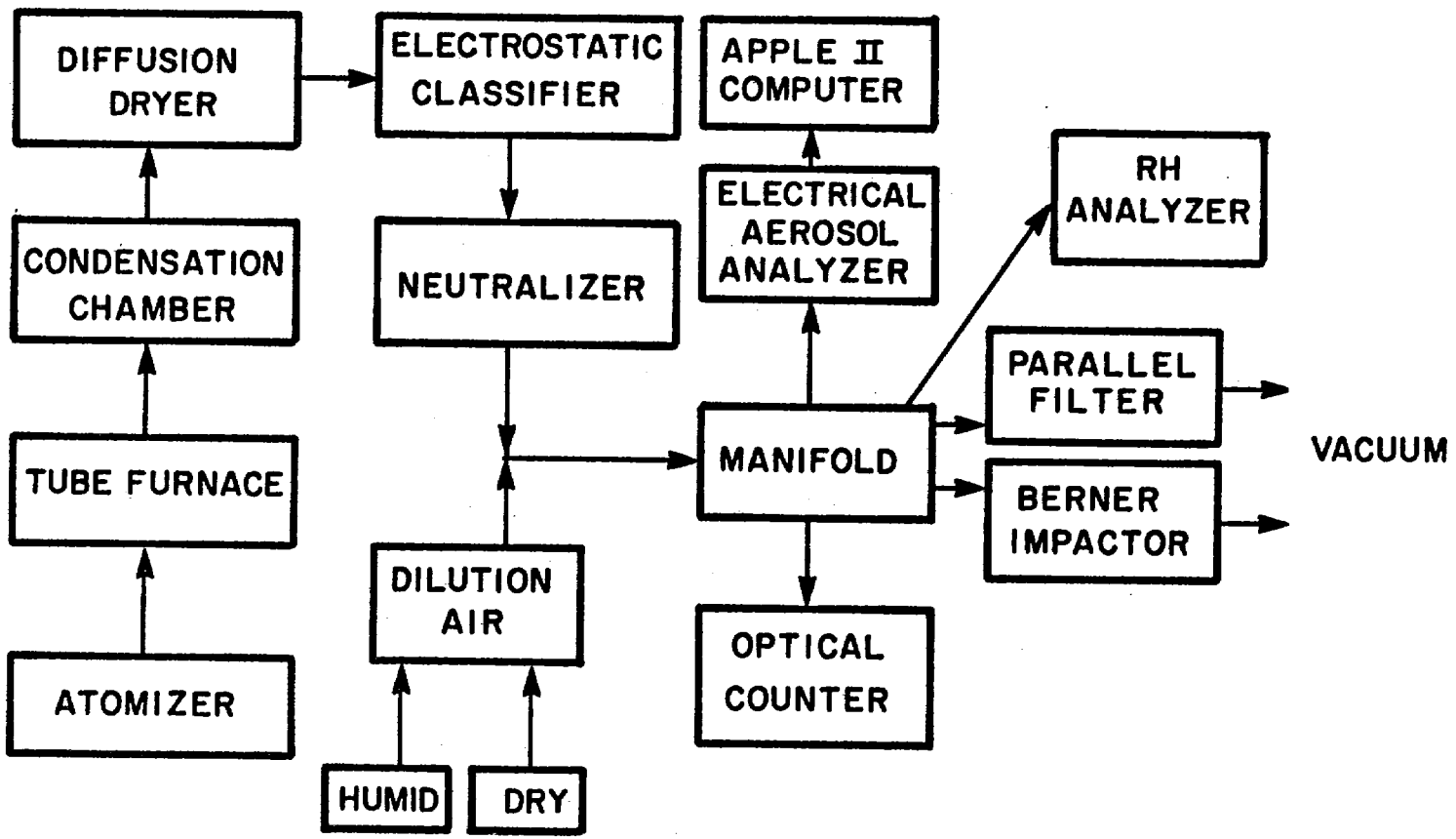

Figure 9. Experimental arrangement for the calibration of the Berner impactor with submicron aerosol.

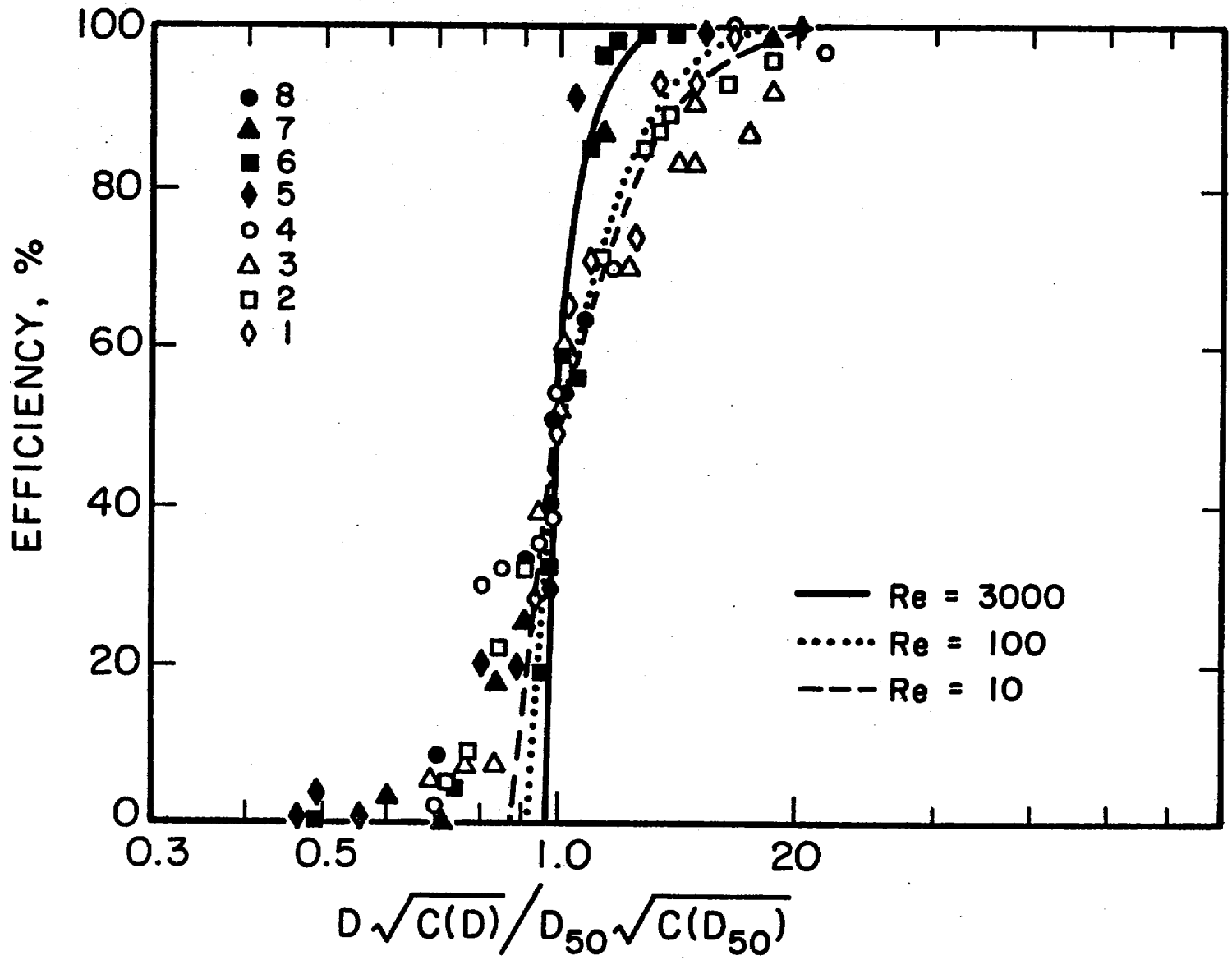

Figure 10. Normalized stage efficiencies of the Berner impactor compared to the theory of Marple for three Reynolds numbers.

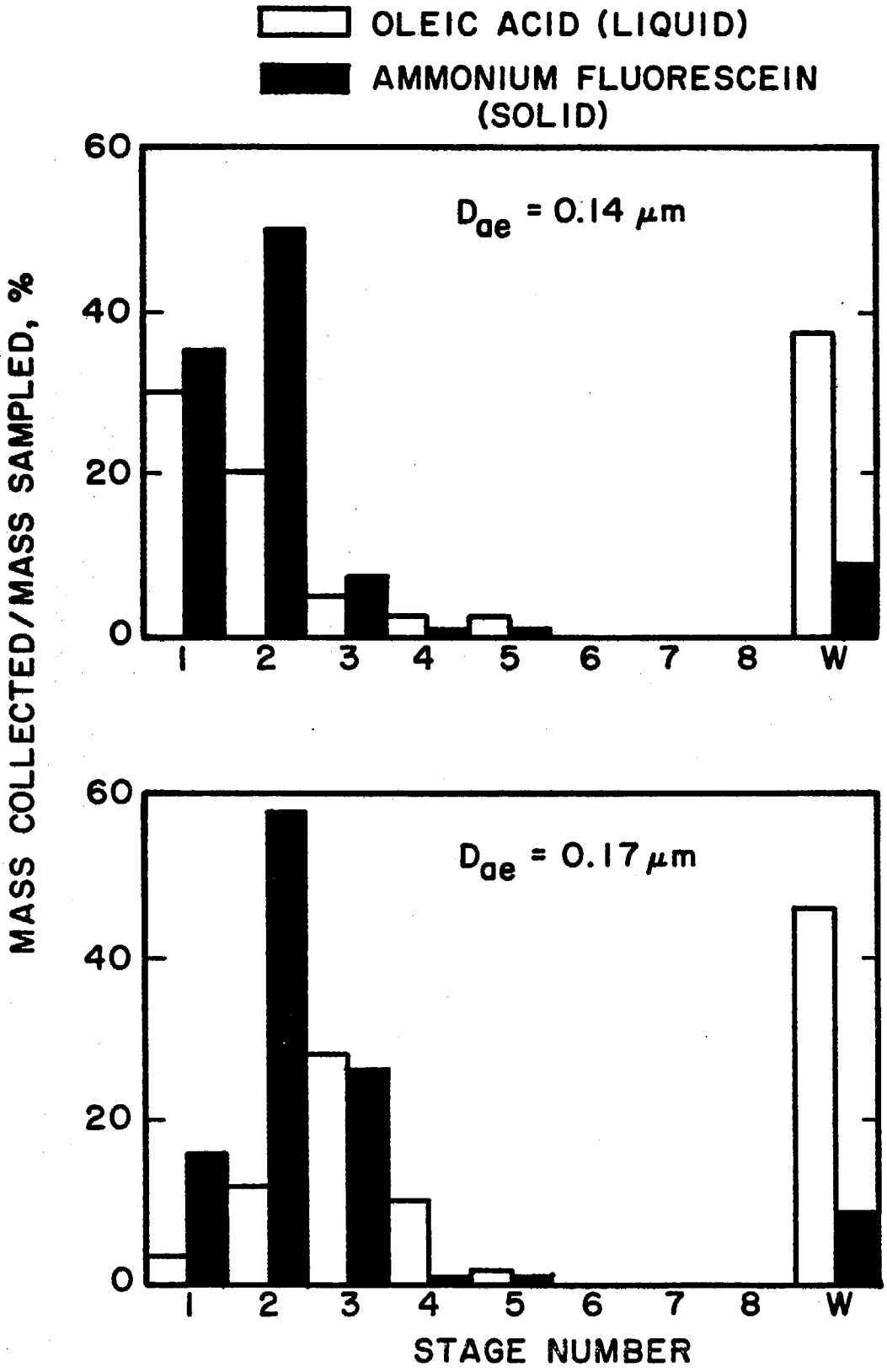

Figure 11. Comparison of the collection of submicron liquid particles with that of oil-coated ammonium fluorescein particles.

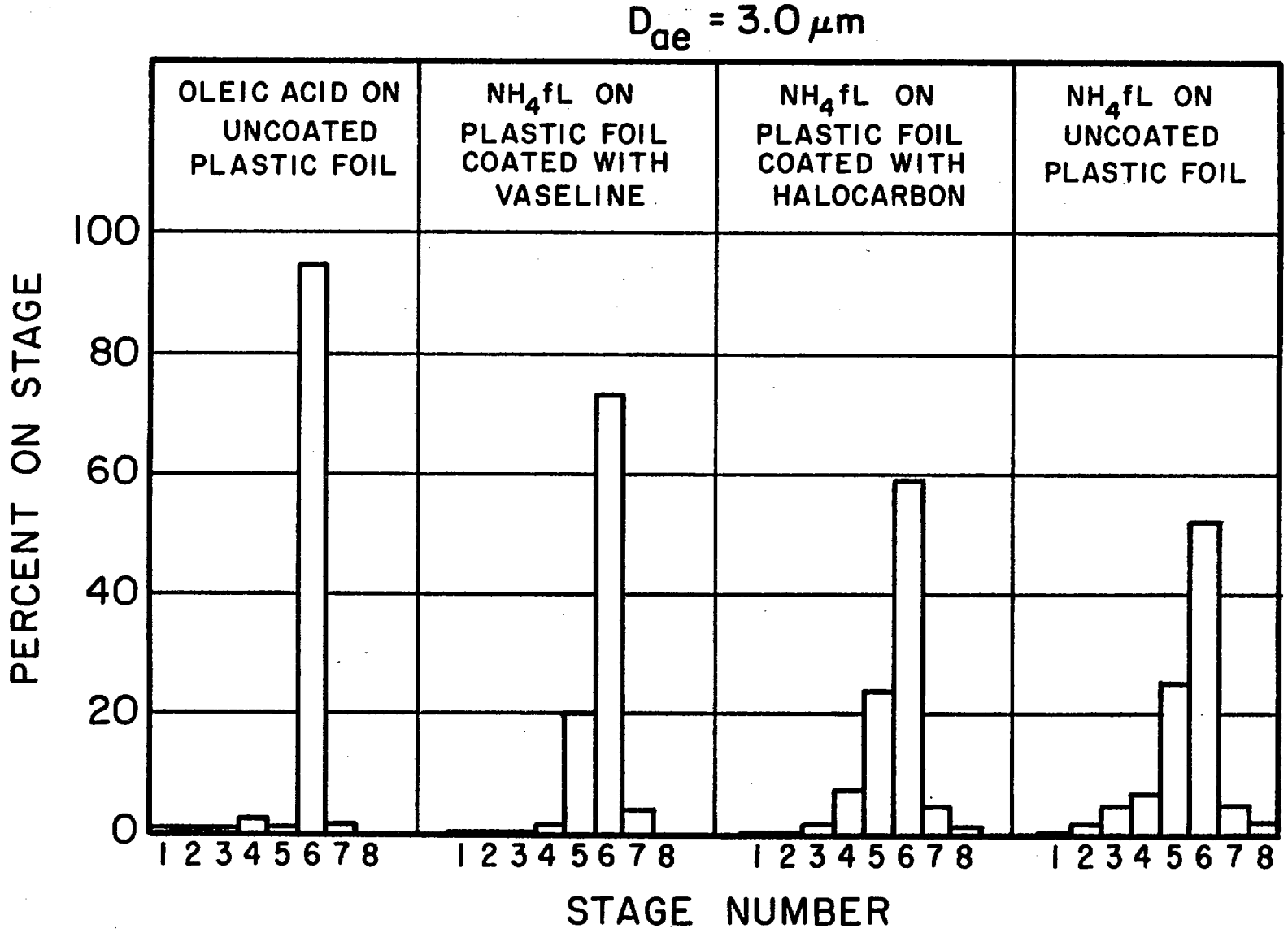

Figure 12. Comparison of the relative stage collections on greased and uncoated substrates.

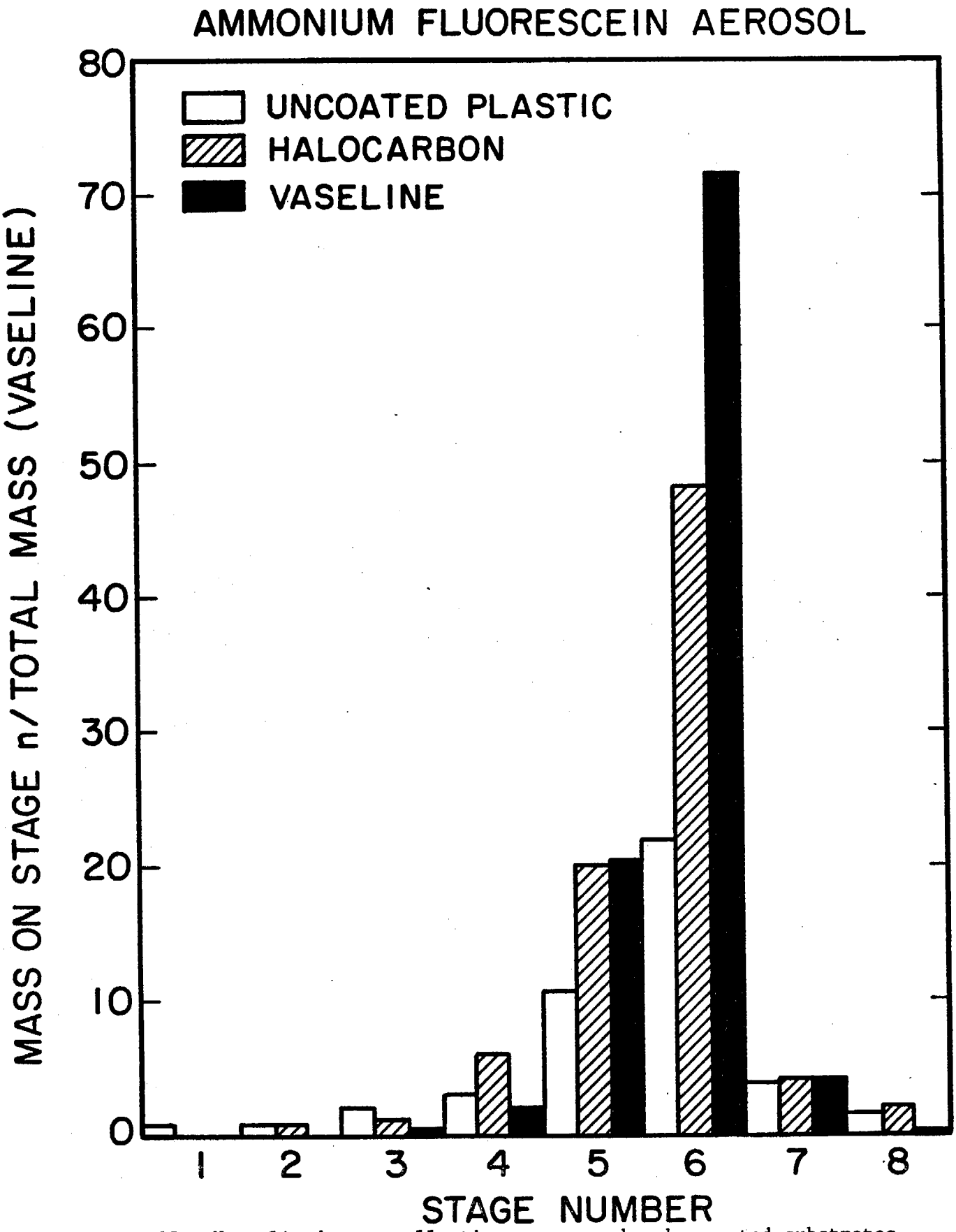

Figure 13. Normalized mass collection on greased and uncoated substrates.

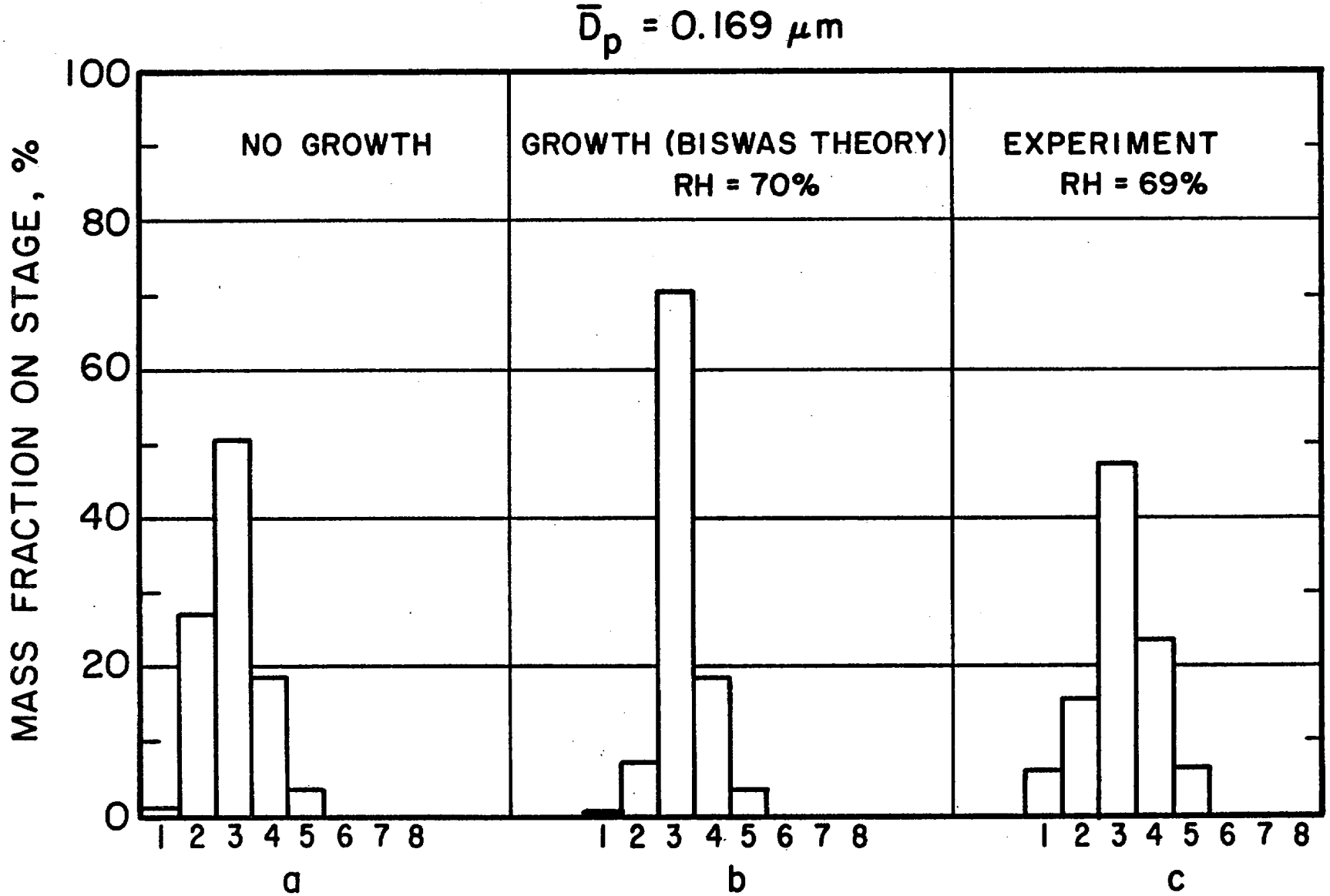

Figure 14. (a) Mass collection on stages for dry aerosol, (b) mass distribution predicted theoretically including growth in particle size when hygroscopic material is sampled at high relative humidity, (c) observed mass distribution of ammonium sulfate sampled at high humidity.

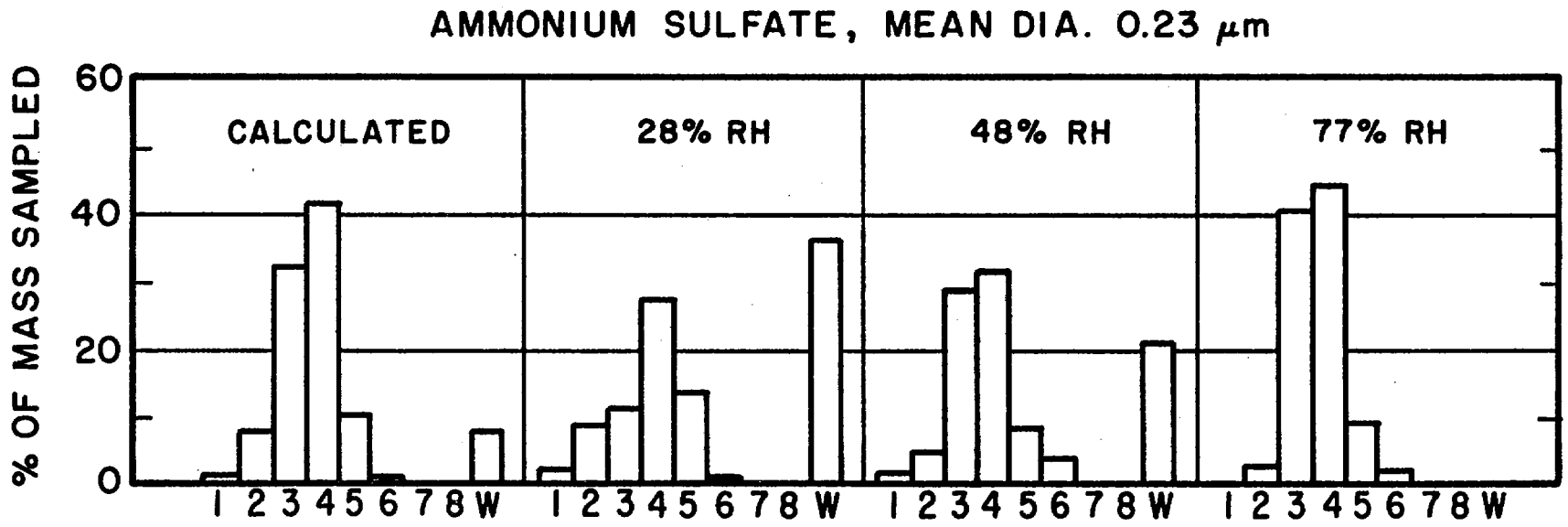

Figure 15. Data taken to investigate bounce of ammonium sulfate particles sampled at different relative humidities.

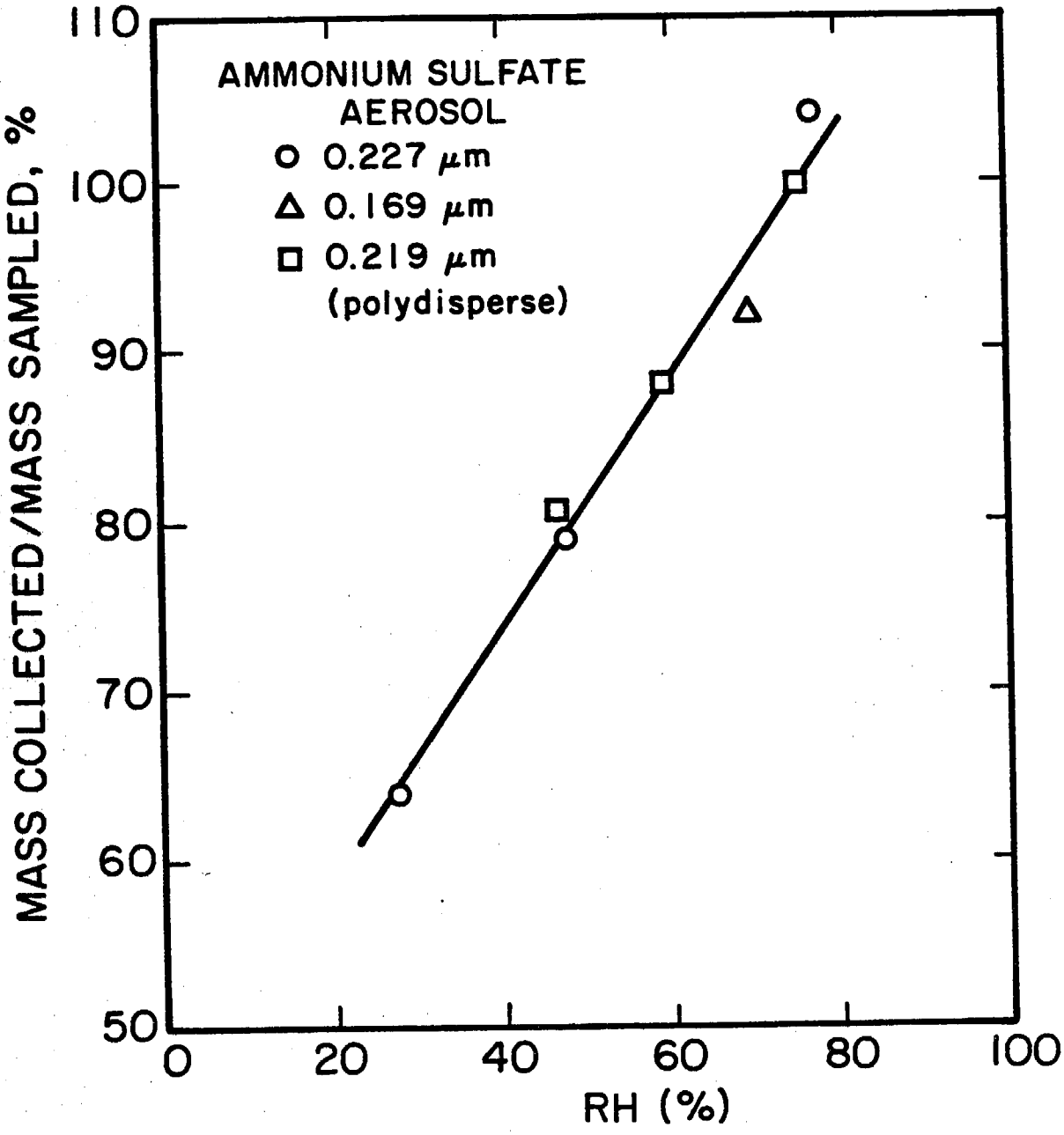

Figure 16. Percentage of ammonium sulfate aerosol collected in the Berner impactor with uncoated Tedlar substrates vs. RH.

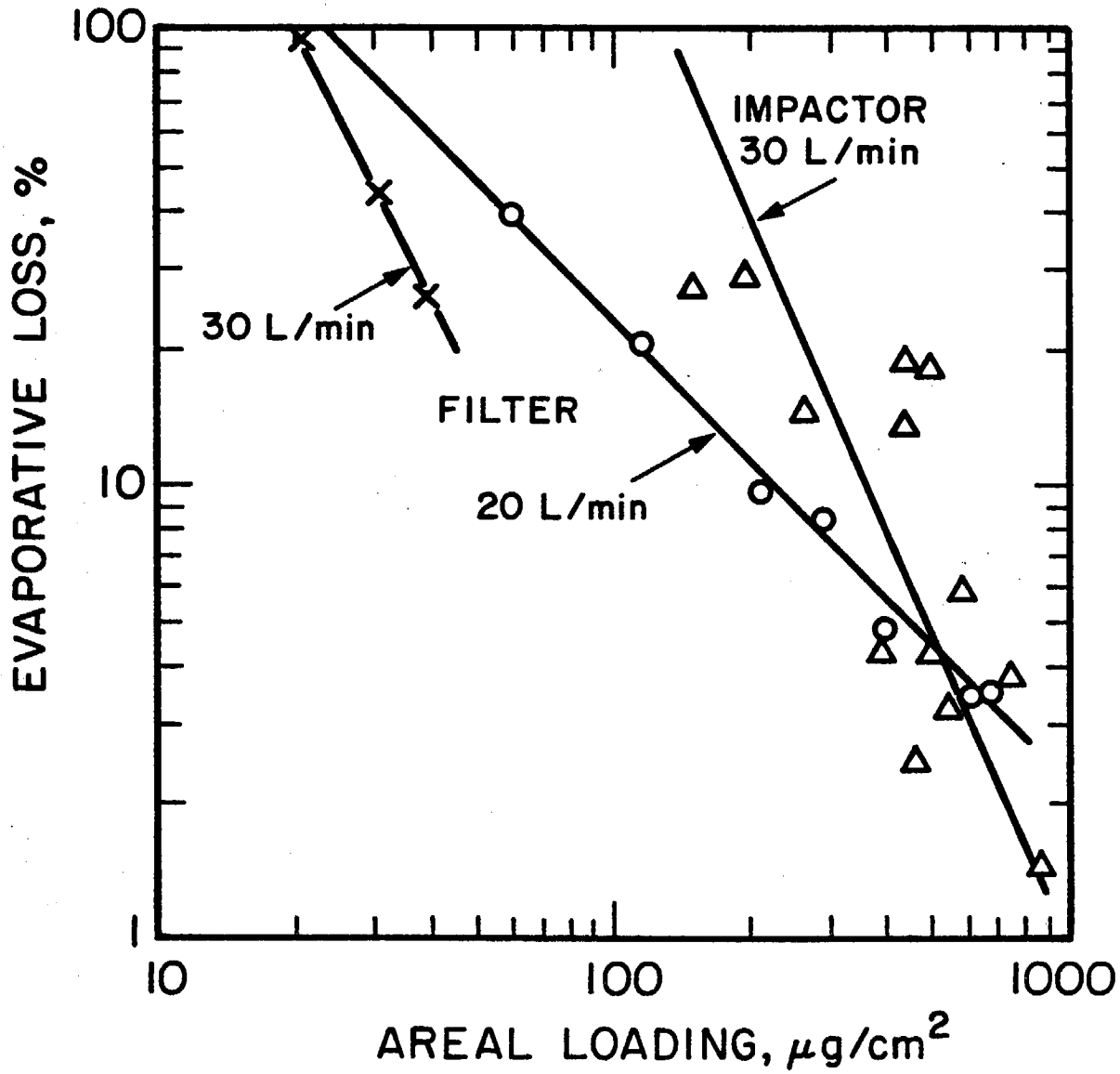

Figure 17. Evaporative loss of ammonium nitrate in the Berner impactor and on a filter vs. areal loading.

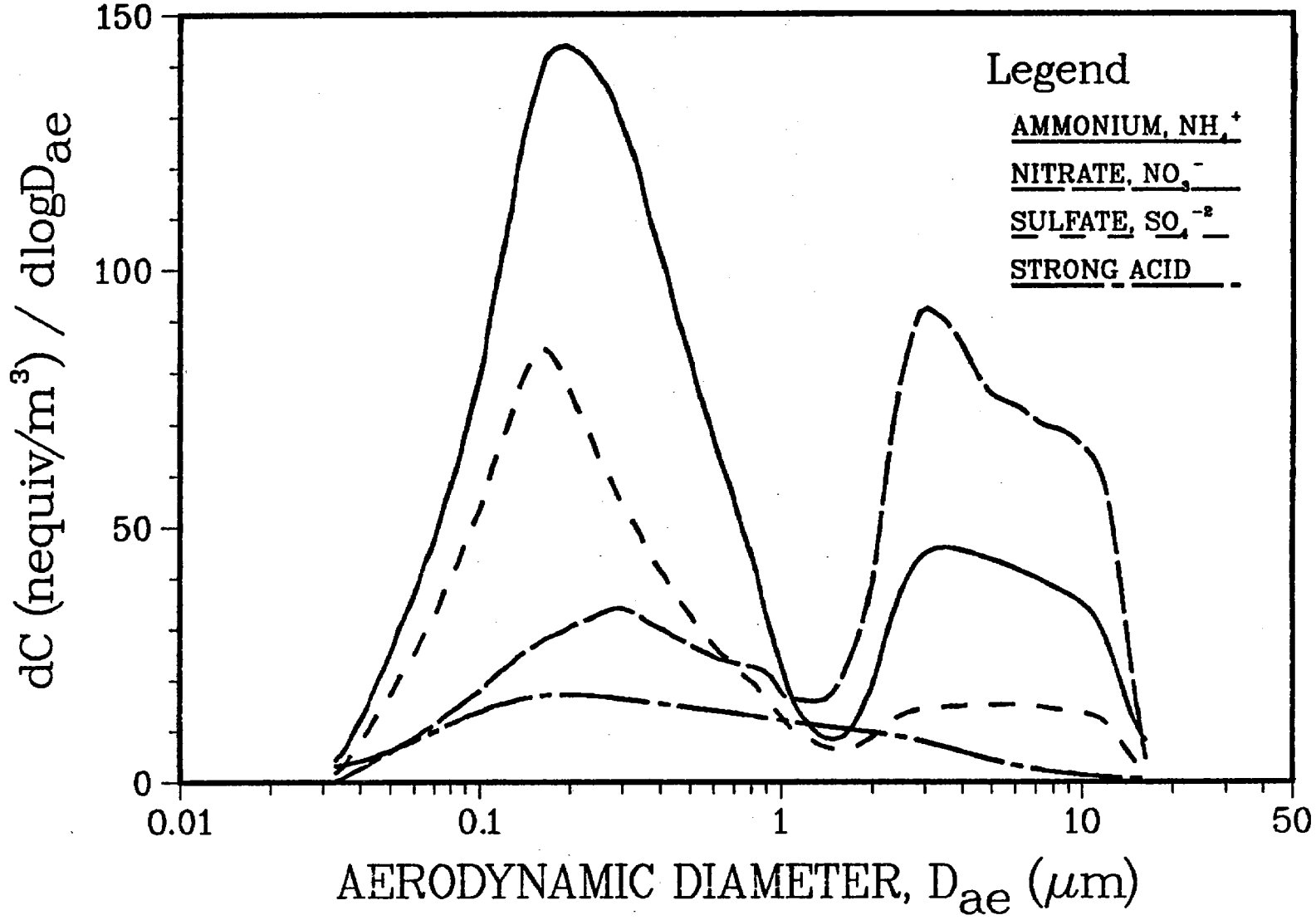

Figure 18. Particle size distributions by chemical species taken in Oildale, Aug. 2-3, 1984.

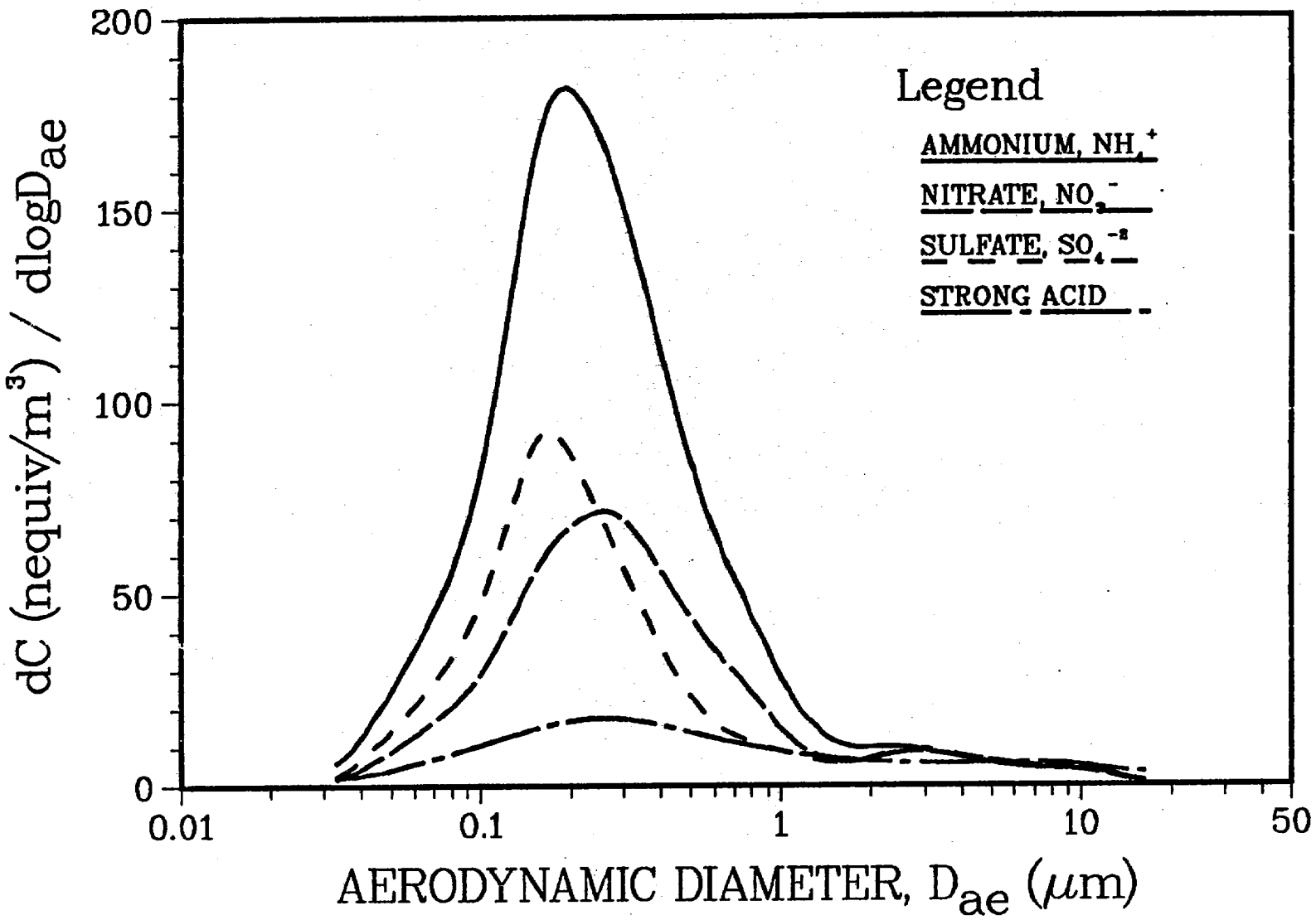

Figure 19. Size distributions in Oildale, Oct. 17-18, 1984.

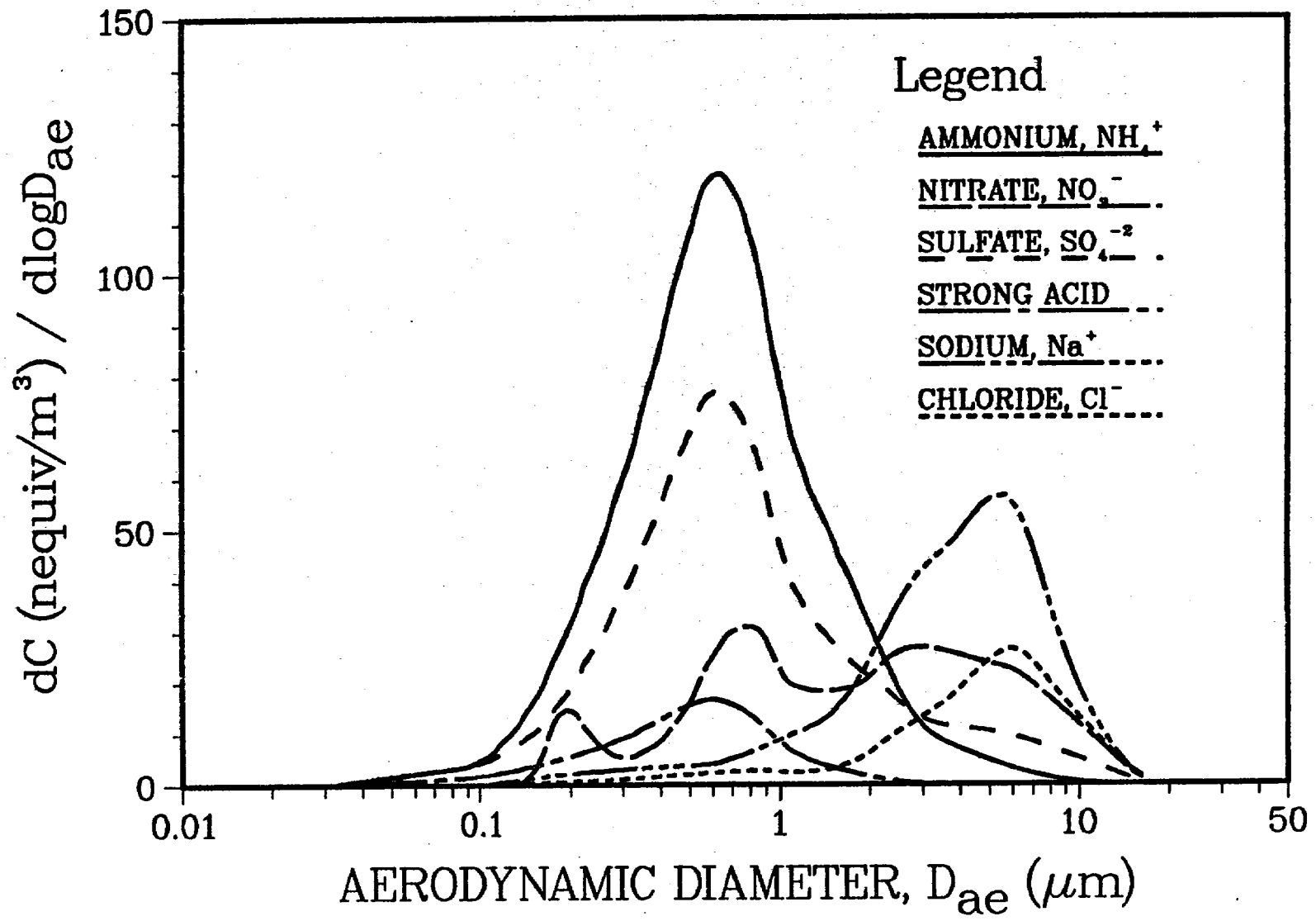

Figure 20. Size distributions in Berkeley, Sept. 25 - Oct. 2, 1985.

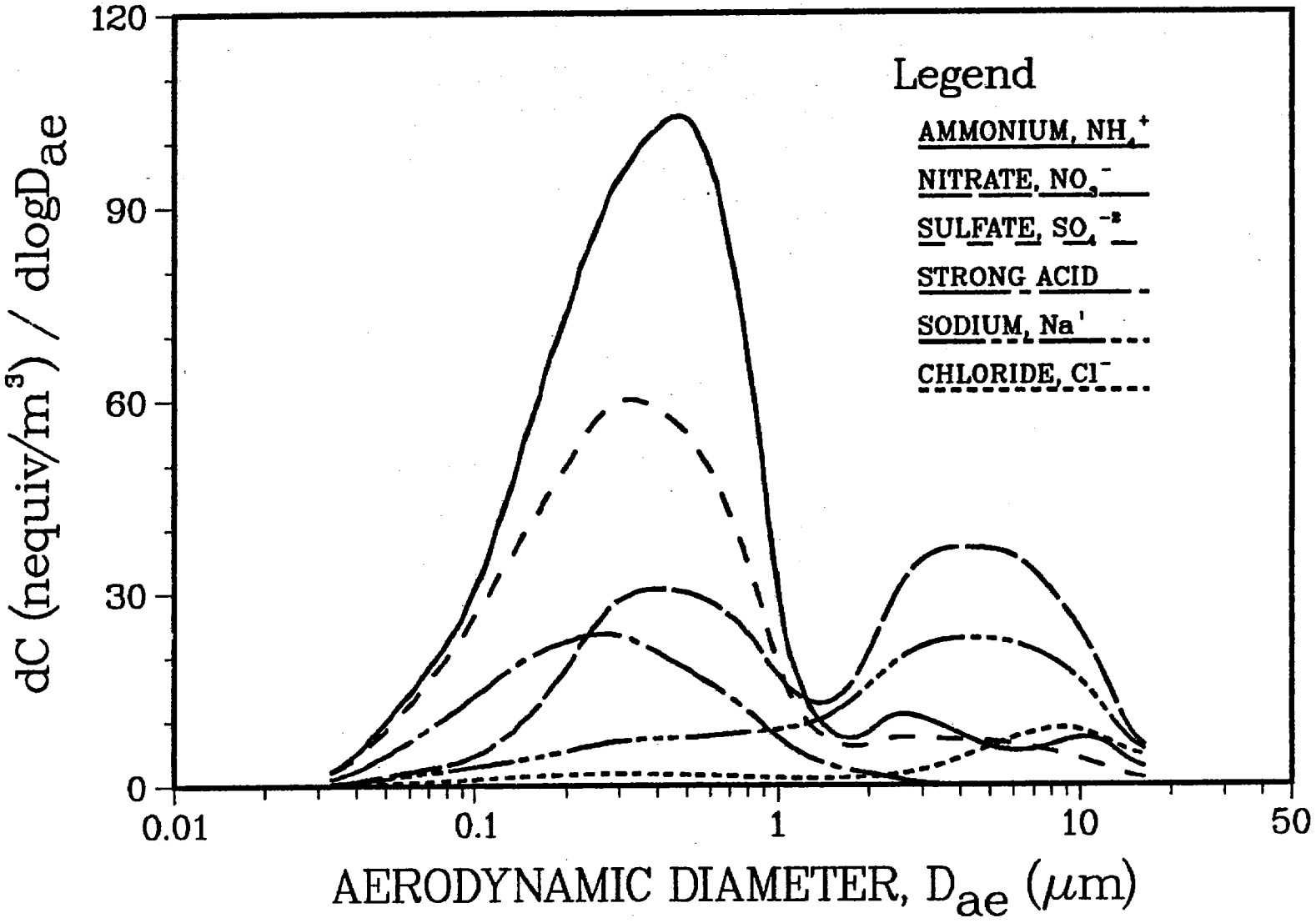

Figure 21. Size distributions in Berkeley, Oct. 2-5,1985.

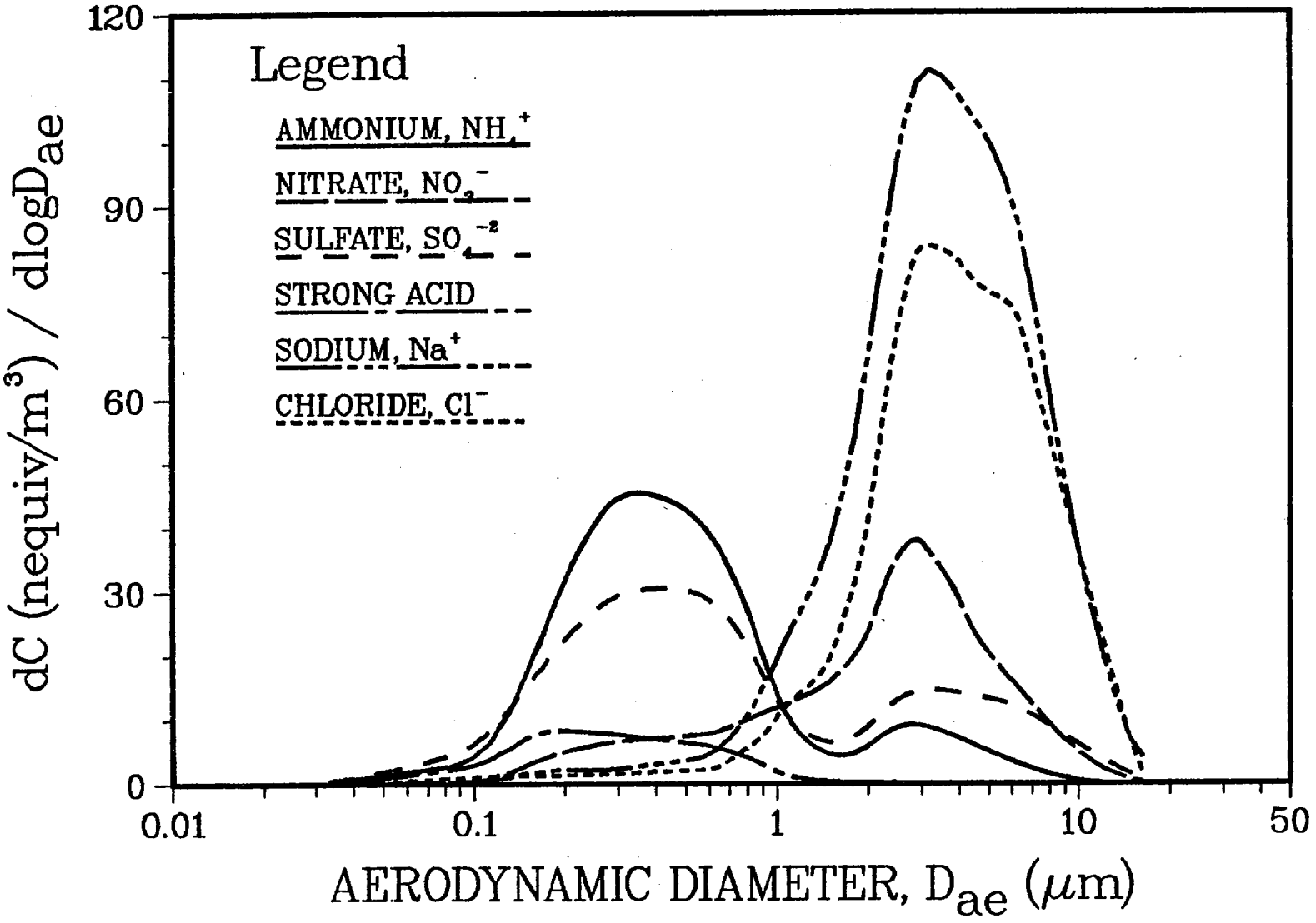

Figure 22. Size distributions in Berkeley, Oct.5-11, 1985.

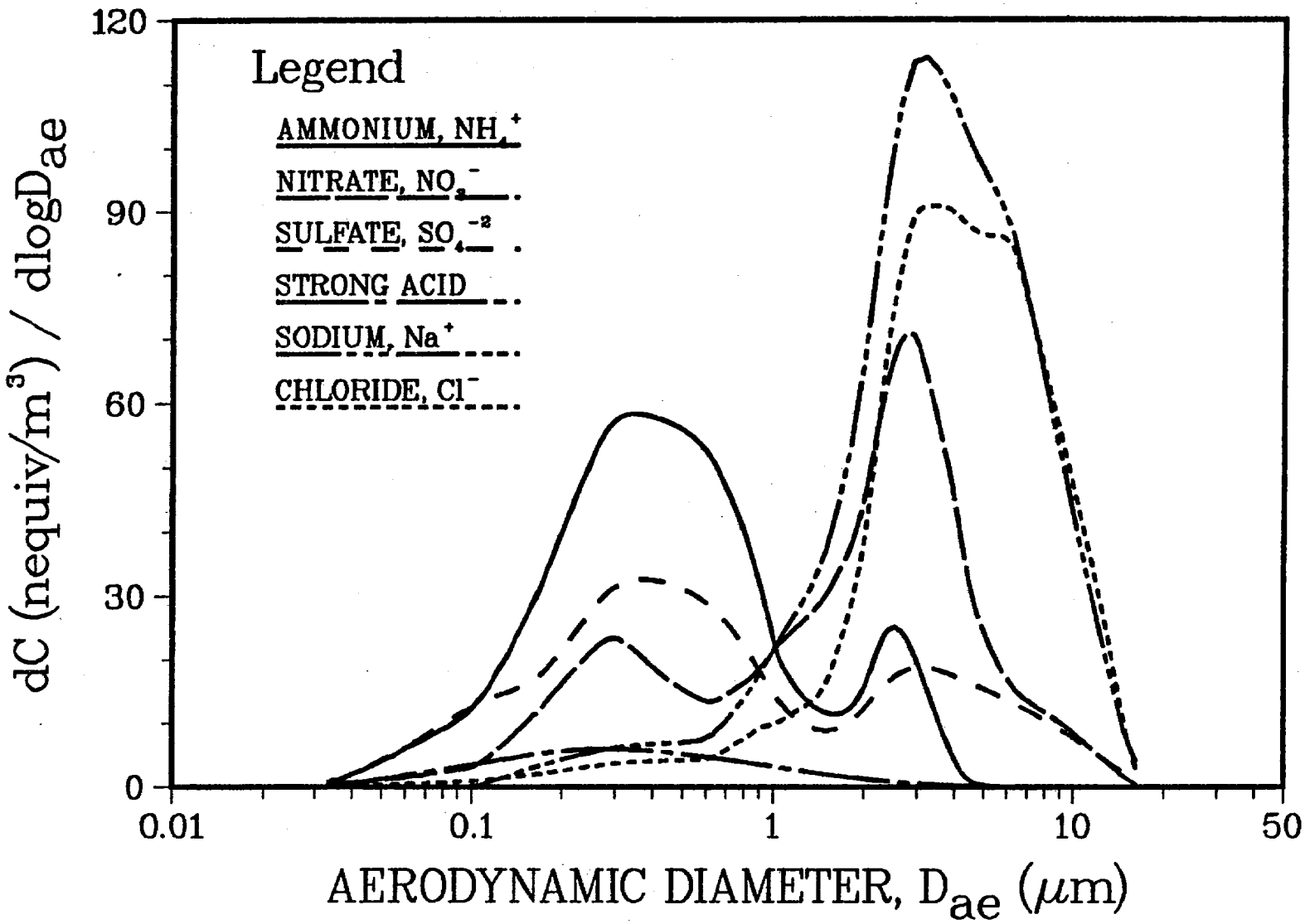

Figure 23. Size distributions in Berkeley, Oct. 14-17, 1985.